UC San Diego
UC San Diego Electronic Theses and Dissertations

Title

Lagrangian Energetics and Vertical Dispersion in Stably Stratified Turbulence

Permalink

https://escholarship.org/uc/item/6qq6r8dh

Author

Jo, Seungbum

Publication Date

2015

Peer reviewed|Thesis/dissertation

UNIVERSITY OF CALIFORNIA, SAN DIEGO

**Lagrangian Energetics and Vertical Dispersion in Stably Stratified
Turbulence**

A dissertation submitted in partial satisfaction of the
requirements for the degree
Doctor of Philosophy

in

Engineering Sciences (Mechanical Engineering)

by

Seungbum Jo

Committee in charge:

      Professor Keiko K. Nomura, Chair
      Professor Jan P. Kleissl
      Professor James W. Rottman
      Professor Kraig B. Winters
      Professor William R. Young

2015

The dissertation of Seungbum Jo is approved, and it is

acceptable in quality and form for publication on micro-

film and electronically:

_____

_____

_____

_____

Chair

University of California, San Diego

2015

DEDICATION

To " my beloved family ".

EPIGRAPH

" Learn, Earn, Return "

These are three phases of life.

- Jack Balousek -

TABLE OF CONTENTS

LIST OF FIGURES

ACKNOWLEDGEMENTS

The completion of my dissertation was possible with the guidance of my committee members, help from friends, and support from my family.

First and foremost I wish to express my deepest gratitude to my advisor, professor Keiko Nomura, for her excellent guidance, caring, patience, and providing me with an excellent atmosphere for doing research. She supported me and my family both financially and emotionally to finish this thesis. She provided me valuable experiences with all the APS talks and I would never forget one of them in Long Beach which gave me an encouragement to welcome a challenge.

I am also very grateful to professor James Rottman for providing me insightful discussions about the research. He was willing to meet and discuss even during weekends. He guided and helped me through the conference presentations, my first presentation in Minneapolis and international conference in Rome.

I also have to thank my committee members, professor Jan Kleissl, professor Kraig Winters, and professor William Young, for their helpful suggestions about the writing and research. Their valuable advice and knowledge became the foundation of my dissertation.

Besides research, I have really enjoyed my teaching experiences at UCSD and gained valuable experiences thanks to all the professors (James Rohr, David Miller, Yousef Bahadori, and Keiko Nomura) I worked with as a TA.

I am very much indebted to my mother, Yanghee Kim, farther, Kwangsub

Jo, mother-in-law, Jungsook Lee, and father-in-law, Baeksoo Kim. They were always supporting me and encouraging me with their best wishes.

A special thanks to my beloved family. Words cannot express how grateful I am to my wife, Jiyang Kim, and two daughters, Sophia Seyeon Jo and Chole Subeen Jo, for all of the sacrifices that they have made on my behalf. They always stood by me through the good times and bad times by cheering me up.

The text of this dissertation includes the reprints of the following papers, submitted for consideration at the time of publication.

Chapter 3: Seungbum Jo, Keiko K. Nomura and James W. Rottman., 'The Lagrangian energetics of a fluid particle in a Boussinesq flow'., in preparation for submission for publication.

Chapter 4: Keiko K. Nomura, James W. Rottman and Seungbum Jo., 'The energetics of vertical fluid particle dispersion in stably stratified turbulence'., in preparation for submission for publication.

VITA

2015	Ph.D. in Engineering Sciences (Mechanical Engineering), University of California, San Diego.
2010	M.S. in Engineering Sciences (Mechanical Engineering), University of California, San Diego.
2004	BS. in Mechanical Engineering, Ajou University, Suwon.

SELECT PRESENTATIONS

Jo, S., Nomura, K. K., Rottman, W. J. 'Energetics of vertical fluid particle dispersion in stably stratified turbulence', (2009) *62nd APS Division of Fluid Dynamics Annual Meeting, Minneapolis, Minnesota.*

Jo, S., Nomura, K. K., Rottman, W. J. 'Energetics of vertical fluid particle dispersion in stably stratified turbulence', (2010) *4th Southern California Symposium on Flow Physics, Irvine, California.*

Jo, S., Nomura, K. K., Rottman, W. J. 'A Lagrangian description of the energetics of stably stratified turbulence', (2010) *63rd APS Division of Fluid Dynamics Annual Meeting, Long Beach, California.*

Jo, S., Nomura, K. K., Rottman, W. J. 'Energetics of vertical fluid particle dispersion in stably stratified turbulence', (2011) *5th Southern California Symposium on Flow Physics, Los Angeles, California.*

Jo, S., Nomura, K. K., Rottman, W. J. 'Energetics of vertical fluid particle dispersion in stably stratified turbulence', (2011) *7th International Symposium on Stratified Flows, Rome, Italy.*

Jo, S., Nomura, K. K., Rottman, W. J. 'The energetics of stably stratified turbulence in the Boussinesq approximation', (2011) *64th APS Division of Fluid Dynamics Annual Meeting, Baltimore, Maryland.*

Jo, S., Nomura, K. K., Rottman, W. J. 'The Lagrangian energetics of stably stratified turbulence in the Boussinesq approximation with non-linear equation of state', (2012) *65th APS Division of Fluid Dynamics Annual Meeting, San Diego California.*

ABSTRACT OF THE DISSERTATION

Lagrangian Energetics and Vertical Dispersion in Stably Stratified Turbulence

by

Seungbum Jo

Doctor of Philosophy in Engineering Sciences (Mechanical Engineering)

University of California, San Diego, 2015

Professor Keiko K. Nomura, Chair

The vertical dispersion of fluid particles in stably stratified homogeneous turbulence with mean shear is investigated. An analysis framework which describes the associated flow energetics in the Lagrangian frame is developed. This provides a more clear and consistent interpretation of the behavior of the mean square vertical displacement, $\sigma_{zp}^2(t)$, which can be related to the total potential energy (TPE) of a given set of fluid particles. The analysis considers TPE in terms of the available potential energy (APE), associated with the nonequilibrium dis-

placement, and the reference potential energy (RPE), associated with the change in particle equilibrium height, i.e., the equilibrium displacement. The corresponding evolution equations describe the key sequence of processes. As fluid particles move away from their equilibrium height, vertical kinetic energy is converted (reversibly) to APE. This establishes nonequilibrium displacement, z' and increases TPE. Without molecular diffusion, gravity will reduce the vertical velocity and the particles will tend to return to their original equilibrium height; APE is converted back to KE in this reversible process. With molecular diffusion, fluid particles will change their density, such to reduce ρ', and therefore, change their equilibrium height, i.e., some of the APE is dissipated and converted to RPE where it accumulates. Molecular diffusion thereby acts to *preserve displacements* and reduce the reconversion of PE to KE. In this manner, fluid particles can move further away from their original equilibrium level and $\sigma_{zp}^2(t)$ can grow without limit.

The evolution equations are integrated in time and give a relation for $\sigma_{zp}^2(t)$. At long time, the RPE will dominate the TPE; $\sigma_{zp}^2(t)$ is then a measure of the total APE dissipated by the flow. The significance of this with respect to the total energy dissipated is given by the cumulative mixing efficiency, Ω_c, which depends on the strength of stratification. In the case of decaying turbulence, $\sigma_{zp}^2(t)$ evolves to a constant value, proportional to Ω_c. In the case of stationary turbulence, the (constant) rate of growth of $\sigma_{zp}^2(t)$ is proportional to Ω_c. The analysis is demonstrated using direct numerical simulations of homogeneous shear flows with decaying, stationary, and growing turbulence. Results for the latter case show $\sigma_{zp}^2(t)$

to continually increase, and to have a reduced dependence on and reduced values of Ω_c as the strength of stratification decreases. In general, simulation results are in agreement with the analysis and confirm that, in homogeneous stratified flows with mean shear, an effective time scale for vertical dispersion at long time is that of the turbulence decay time.

Chapter 1

Introduction

1.1 Introduction

Air quality is controlled by how effective atmospheric turbulence can disperse gaseous and particulate pollutants released at the earth's surface. Because of its vital importance, there have been significant efforts to develop simple and effective models of turbulent dispersion for air quality applications [65]. However, current dispersion models are found to be weak in their ability to predict dispersion in the stable boundary layer which is characterized by turbulence, stratification, internal waves and shear [36]. This is due in part to some uncertainties in the understanding and modeling of the physics of turbulent dispersion in stably stratified conditions.

In a neutrally stratified flow, buoyancy forces do not restrict the vertical motion of fluid particles and they can move vertically over unlimited distances by

advection. In a stably stratified turbulent flow, the vertical motion of fluid particles are restricted by buoyancy forces. If there is no molecular diffusion, the density of fluid particles does not change and they are constrained to oscillate about their equilibrium level. If molecular diffusion is considered, an interchange of density will cause fluid particles to change the equilibrium level of their oscillations. The fluid particles can thereby move further away from their original equilibrium levels. The overall turbulent dispersion is then a result of two processes: large-scale turbulent advection and small-scale molecular mixing [40]. The relative importance of each process and the range of conditions under which each process dominates is not clear.

Turbulent dispersion can be investigated in terms of energetics since the vertical displacement can be considered in terms of potential energy. Large-scale turbulent advection can establish overturns that raise a heavy fluid above a light fluid which results in an increase in potential energy (PE). The associated kinetic energy (KE) is converted to available potential energy (APE), which is the portion of PE, available for conversion back to KE. However, molecular diffusion will cause density changes and APE is dissipated. Eulerian energetics developed by Winters et al [68] has been used to describe the advection and molecular diffusion. However, energetics in the Lagrangian frame, which is more appropriate framework to investigate fluid particles' dispersion, has not been fully developed.

This study considers stably stratified homogeneous shear flow, the simplest flow that contains turbulence, shear and stratification, to investigate the physics

of mixing and dispersion.

1.2 Literature Review of Research

1.2.1 Turbulent Dispersion in Stratified Flow

Fundamental analyses of turbulent dispersion are based on the statistical theory developed by Taylor for stationary, homogeneous turbulence in an unstratified fluid [57]. Taylor's diffusion theory is based on the statistical theory of Brownian motion, where random movements of particles are only due to collisions. An ensemble average of the displacement of particles is given by

$$\langle \sigma_i^2 \rangle = 2\langle u_i^2 \rangle \int_t^{t_o} (t - \tau) R_{ii}(\tau) \, d\tau \tag{1.1}$$

where $\langle \ \rangle$ denotes ensemble averages, σ_i is a displacement from an initial position, u_i is the vertical fluctuating velocity and t is the travel time from the source. The mean square of particle displacement is directly related to the Lagrangian velocity autocorrelation function which is given by

$$R_{ii}(\tau) = \frac{\langle u_i(t) u_i(t + \tau) \rangle}{\langle u_i^2 \rangle} \tag{1.2}$$

In a stationary process, the mean square dispersion at short time can be obtained by assuming $R_{ii}(\tau = 0) \approx 1$ from (1.1).

$$\langle \sigma_i^2 \rangle = \langle u_i^2 \rangle t^2 \tag{1.3}$$

After a long enough time τ, the particle forgets its initial velocity. Therefore, $u_i(t + \tau)$ is independent of $u_i(t)$ and $\langle u_i(t)u_i(t + \tau) \rangle \rightarrow 0$. As fluid particle velocities decorrelate from their original values, the mean square displacement increases linearly with time.

$$\langle \sigma_i^2 \rangle = \langle u_i^2 \rangle T_{L,ii} t \tag{1.4}$$

where $T_{L,ii} = \int_\infty^0 R_{ii}(\tau)\, d\tau$ is the Lagrangian integral timescale. Therefore, in neutrally stratified flows, fluid particles can move vertically over unlimited distances. Large-scale vertical dispersion is relatively insensitive to small-scale mixing and in most calculations of turbulent dispersion in neutrally stratified fluids, molecular mixing is not considered.

In stably-stratified fluids, if the density of the fluid particles remains unchanged, it can be shown (assuming stationary turbulence and equipartition of kinetic and potential energies) that fluid particles are constrained to oscillate about their equilibrium density level a vertical distance of order σ_w/N, where σ_w is the rms vertical component of turbulent velocity and N is the local buoyancy frequency of the fluid [7, 40]. However, molecular diffusion alters the density of fluid particles which, in turn, alters the equilibrium level about which they oscillate, the fluid particles may move farther away from their former equilibrium levels. This is the physical description developed by Pearson, Puttock and Hunt [40], hereafter referred to as PPH. They consider the vertical flux of density, in Lagrangian terms, to consist of two components: that associated with the growth in vertical displace-

ment of fluid particles and that associated with the change in particle density due to molecular diffusion. PPH claim that, while in neutrally stratified flows the former component dominates, in stably-stratified flows the latter becomes significant due to the constraints on the former [18]. As stratification increases, mixing may then become the dominant transport mechanism and thereby alter the nature of the diffusivity.

PPH extend the earlier work of Csanady [7] to develop a mathematical model of vertical dispersion in stably-stratified stationary turbulence based on Langevin-type equations. In their model, the rate of change of density of fluid elements by molecular mixing is explicitly accounted for and described by,

$$\frac{d\rho}{dt} = \kappa \nabla^2 \rho = -\gamma N \rho' \tag{1.5}$$

where the mixing parameter, γ, is the ratio of the buoyancy timescale to the diffusion timescale. Results of the model show that, for small times, $Nt << 1$, the mean squared vertical displacement of fluid elements, $\sigma_z^2(t)$, behaves as that in neutrally stratified fluid (1.3),

$$\sigma_z^2(t) = \sigma_w^2 \, t^2 \ . \tag{1.6}$$

For longer times, $Nt > 1$, the model prediction is given by,

$$\sigma_z^2(t) = (\sigma_w/N)^2 \, (\zeta_z^2 + 2\gamma^2 \, Nt) , \tag{1.7}$$

where ζ_z is a dimensionless parameter of order unity which depends on the shape of the turbulent pressure gradient spectrum. Thus, the behavior of $\sigma_z^2(t)$ is dependent

on the value of the mixing parameter γ. If $\gamma << 1$, $\sigma_z^2(t)$ may exhibit nearly constant values (dispersion plateau) for intermediate times, $1 < Nt < \gamma^{-2}$. For large γ, or large times $Nt >> \gamma^{-2}$, the model predicts a slow linear growth, $\sigma_z^2 \sim t$. Values of the mixing parameter are found to be in the range, $0.1 \leq \gamma \leq 0.4$, which yield both types of behavior [18]. In order to account for the effects of shear, an ad-hoc parameterization of γ is used [19].

On the other hand, Venkatram, Strimaitis, and Dicristofaro [63], hereafter referred to as VSD, present a semi-empirical model to estimate vertical dispersion based on the assumption that molecular mixing effects are negligible. According to their model, at long time, σ_z^2 exhibits a linear growth without an intervening constant period. These two models are based on fundamentally different interpretations of the importance of molecular mixing in turbulent dispersion and they produce significantly different results. Das and Durbin [9] have formulated a Lagrangian stochastic model for turbulent dispersion that accounts for shear and inhomogeneities in stratified flows but the validation of these models is limited.

Direct numerical simulations (DNS) have been performed to study turbulent dispersion in homogeneous stably stratified unsheared flows. Results for decaying (unforced) turbulence [24, 22, 62] show that σ_z^2 evolves in time to a constant value, which scales approximately with N^{-2}. Results for stationary (forced) turbulence [60, 5] show a linear growth in σ_z^2 at long time, supporting the PPH model prediction. A plateau at intermediate times is also observed in these results at sufficiently low buoyancy Reynolds numbers, $Re_b = \varepsilon_k/(\nu N^2)$, and Froude

numbers, $Fr = \varepsilon_k/(N E_k)$, where E_k and ε_k are the turbulent kinetic energy and its dissipation rate, respectively [5].

Venayagamoorthy and Stretch [62] (hereafter referred to as VS) examine the physical ideas of PPH and the significance of small-scale mixing on particle dispersion by tracking and evaluating the mixing of fluid particles in their DNS. They find that in weakly (and neutrally) stratified flows, mixing limits the density perturbation of fluid particles. As stratification increases, mixing is suppressed and the density perturbations become controlled by advection consistent with the predominance of oscillating wave motion. They attempt to quantify the significance of mixing through a decomposition of the vertical displacement in terms of an isopycnal (adiabatic) displacement, i.e., the deviation from the particle equilibrium level with respect to the background mean density profile, and a diapycnal (diabatic) displacement, i.e., the change in the particle equilibrium level due to the change in its density. They find that the diapycnal displacement dominates the total displacement even in weakly stratified flows. In general, the observed significance of the effects of mixing supports the basic underlying ideas of PPH. However, VS find that the timescale for density changes due to mixing does not scale well with that of buoyancy, as proposed by PPH (1.5), but instead with the energy decay timescale.

Lindborg and Brethouwer [29] (hereafter referred to as LB) derive expressions for $\sigma_z^2(t)$ for both decaying and stationary turbulence by integrating the evolution equation for density fluctuations and applying turbulence scaling argu-

ments and, in particular, they assume the mixing time to be comparable with the Kolmogorov time scale. Their results for decaying flows at long time predicts σ_z^2 to become constant, as observed in the DNS studies. The constant value is shown to be $2(E_{ap}(0)+aE(0))/N^2$, where $E_{ap}(0)$ and $E(0)$ are the initial turbulent potential and total (kinetic and potential) energies and $0 < a < 1$. Their result for stationary flows at long time predicts $\sigma_z^2 = (4E_{ap} + 2\,\varepsilon_P\,t)/N^2$, where ε_P is the turbulent potential energy dissipation rate. LB interpreted the first term as the adiabatic contribution to the mean square vertical displacement and the second term as the diabatic contribution to the mean square vertical displacement. Comparisons with their DNS of forced stationary turbulence [5] show good agreement of the development of the plateau at intermediate times, associated with the adiabatic contribution, and linear growth at long time. The long time growth rate agrees with VS that the relevant time scale is the turbulence decay time. Although the results of Lindborg and Brethouwer [29] provide quantitative predictions for $\sigma_z^2(t)$, the physical interpretations are still not entirely clear since $\sigma_z^2(t)$ was derived in an indirect manner. In particular, although energy quantities, i.e., turbulent kinetic and potential energies, appear in their result, they do not explicitly consider the energetics of the dispersion process. A more complete and systematic analysis of the energetics of turbulent dispersion in stably stratified flow needs to be developed.

1.2.2 Energetics of Stably Stratified Flow

The energetics of stratified flow is usually formulated in the Eulerian framework. Here, we review the analysis developed by Winters *et al.*[68]. The total potential energy (TPE) for a volume of fluid is defined as

$$E_p \quad = \quad g \int \rho z \, dV \qquad (1.8)$$

where ρ is the density of the fluid and z is the vertical spatial coordinate.

Since not all of the TPE is available for conversion into KE, it is more useful in considering energetics, to decompose the PE into an available part and a non-available part. The component of PE available for conversion to KE is the Available Potential Energy (APE). The other component of PE is the background potential energy (BPE) which is defined as the minimum potential energy attainable through adiabatic redistribution of the density and given by,

$$E_b \quad = \quad g \int z_*(x,t)\rho(x,t) \, dV \qquad (1.9)$$

where z_*, obtained from an actual state through an adiabatic rearrangement, is the vertical reference position in the state of minimum gravitational potential energy at a given point (x,t) and defined as $z_*(x,t) = \frac{1}{A} \int H[\rho(x',t) - \rho(x',t)] \, dV'$ and H is the Heaviside step function.

Then, APE is obtained by subtracting BPE (1.9) from TPE (1.8),

$$E_a \quad = \quad E_p - E_b \quad = \quad g \int \rho(z - z_*) \, dV \qquad (1.10)$$

This concept of APE was first introduced by Margules [32] and developed by Lorenz [31]. Lorenz's APE is defined as the difference in the potential energy between actual and reference state and is the available part of TPE for conversion to KE which is eventually transformed to background potential energy via molecular mixing. Equations (1.9) and (1.10) explicitly define APE and BPE for Eulerian energetics.

The evolution equations of KE, APE and BPE for a closed system are given by,

$$\frac{dE_k}{dt} = -\Phi_z - \varepsilon_k \tag{1.11}$$

$$\frac{dE_a}{dt} = \Phi_z - \Phi_d + \Phi_i \tag{1.12}$$

$$\frac{dE_b}{dt} = \Phi_d \tag{1.13}$$

where E_k is a kinetic energy, ε_k is a viscous dissipation of kinetic energy, $\Phi_z = \int g\rho w \, dV$ is the buoyancy flux which can be converted into kinetic energy reversibly, $\Phi_d = \kappa g \int -\frac{dz_*}{d\rho}(\nabla\rho)^2 \, dV$ is the dissipation rate due to diffusion, $\Phi_i = -\kappa g A(\overline{\rho}_{top} - \overline{\rho}_{bottom})$ is the conversion rate from internal energy to potential energy, κ is the thermal diffusivity, A is the fixed horizontal area and $\overline{\rho}_{top}$ and $\overline{\rho}_{bottom}$ is the horizontal mean density of top surface and bottom in ocean respectively.

In the Lagrangian point of view, an expression for the locally defined APE density (hereafter defined as E_{ap}) for the case of an incompressible fluid with arbitrary stratification and adiabatic processes was proposed by Holliday and McIntyre [14] and Andrews [1] showed that the results hold for a compressible fluid. The

APE density is defined as the integral of the displacement of a fluid particle from its equilibrium state and given by,

$$
\begin{aligned}
E_{ap} &= -\int_0^\zeta g\hat{\zeta}\rho_o'(z-\hat{\zeta})\,d\hat{\zeta} \\
&= \rho(z-\zeta)g\zeta + P(z) - P(z-\zeta)
\end{aligned}
\tag{1.14}
$$

where $\hat{\ }$ denotes a dummy integration variable, ζ is the vertical displacement of fluid particle from its original, undisturbed position, $z - \zeta$ is an original, undisturbed position, ρ_o' is the derivative of undisturbed density with respect to height z and, $P(z)$ and $P(z-\zeta)$ are the hydrostatic pressure at z and $z - \zeta$. Equation (1.14) shows the sign positive definite APE.

Although Roullet & Klein [44] and Molemaker & McWilliams [33] considered the presence of molecular diffusion, only the APE density was defined. The PE quantity comparable to BPE has not been considered for Lagrangian energetics. Therefore, the full Lagrangian energetics needs to be established to describe the motion of fluid particles with molecular diffusion.

1.3   Summary and Outstanding Issues

As discussed in the previous section, current dispersion models are based on two statistical theories for dispersion. One is the PPH model which extends Csanady's idea and accounts for small-scale mixing by describing the molecular diffusion in terms of changes in the equilibrium level of the particles. The other is the VSD model, which neglects molecular diffusion and is based on an extension

of Taylor's standard statistical theory. Due to the different interpretations of the importance of mixing in turbulent dispersion, those two models produce significantly different results. For short time, they agree but for long time, according to the PPH model, the turbulent dispersion is dependent on the mixing parameter γ but VSD model shows that the behavior of $\sigma_z^2(t)$ grows only linearly in time and a mixing parameter is constant. LB derive the equations for $\sigma_z^2(t)$ for stationary and decaying turbulence but the equations are derived in an unclear manner. The outstanding issues include the interpretation of molecular diffusion effects on turbulent dispersion and the dependence of the behavior of mean square vertical displacement on the value of the mixing parameter.

In the energetics study, the Eulerian energetics analysis has been used to investigate the mixing process and diabatic effects but a Lagrangian frame is more appropriate for dispersion modeling because it explicitly considers the vertical displacement of fluid particles. However, currently only the APE component is developed for Lagrangian energetics and a total PE description is not fully developed.

1.4   Research Objectives

The overall objective of this research is to better understand and predict vertical fluid particle dispersion in a stably stratified turbulent flow, in particular, to clarify the role and significance of molecular diffusion.

In order to accomplish the objective, we consider the energetics of the fluid particles and relate potential energy (PE) components to the mean square vertical displacements. The time development of the potential energy components will then provide a clearer description of the physics of fluid particle motion with a diabatic effect. Specific objectives of the study include:

- Develop a Lagrangian analysis of the PE energetics.

  - Previously, APE was the only potential energy component that had been defined in the Lagrangian framework. Here, we will define a new energy quantity, the reference potential energy (RPE), which we will show is the Lagrangian equivalent of BPE.

  - We will develop the associated evolution equations and investigate the underlying physics. This will clarify the role and significance of mixing process.

- Derive expression for $\sigma_z^2(t)$ from the PE evolution equations and interpret fundamental physics of vertical dispersion.

  - The PE components will be expressed in terms of mean square vertical displacements and the mixing effect investigated by comparing the equilibrium and nonequilibrium PE component. The relative significance of stirring and mixing will be evaluated and a proper timescale associated with turbulent dispersion determined.

- Demonstrate the developed results using DNS.

  - DNS is performed for three flow conditions, decaying, stationary, and growing turbulent flow to confirm the analytical results of the energetics and vertical dispersion.

1.5 Dissertation Outline

The content of this dissertation is arranged into five further chapters:

- Chapter 2 provides the flow description for the analysis, including the definitions of basic parameters and governing equations for the Boussinesq flow.

- Chapter 3 presents the development of the Lagrangian energetics. Potential energy components and their associated time evolution equations are considered. A physical interpretation of each conversion terms is investigated.

- Chapter 4 develops a turbulent dispersion model by applying the Lagrangian energetics. The appropriate dispersion timescale and relations are proposed and compared with existing models. Three flow conditions including decaying, stationary, and growing flow, are examined to investigate the mixing effect on dispersion.

- Chapter 5 presents the DNS results demonstrating the energetics analysis of turbulent dispersion in homogeneous stably stratified shear flow.

- Chapter 6 concludes this dissertation with a summary of significant results of this research. Suggestions for further work are indicated.

- Appendix A describes the numerical methodology for DNS. The particle tracking algorithm is also described to obtain Lagrangian statistics.

Chapter 2

Basic Flow Description

2.1 Physical Description

Our primary application of interest is turbulent dispersion in the atmosphere under stably stratified condition. We therefore consider the motion of fluid particles in an unbounded domain. A uniform background stable stratification $(d\overline{\rho}/dz < 0)$ is imposed which is fixed in time. Buoyancy effects due to gravity are important. Flow velocities are much smaller than the speed of sound so that the density change due to pressure changes is small compared to that due to temperature changes, hence, the equation of state is $\rho = f(T)$. The fluid is a gas and assumed to behave as an ideal gas.

The dependent variables of interest in this study are velocity vector $\boldsymbol{v}$, pressure p, temperature T and density ρ. The instantaneous position and velocity

vectors are given by,

$$\boldsymbol{x}(x, y, z, t) \quad = \quad (x_1, x_2, x_3) \quad = \quad (x, y, z) \tag{2.1}$$

$$\boldsymbol{v}(x, y, z, t) \quad = \quad (u_1, u_2, u_3) \quad = \quad (u, v, w) \tag{2.2}$$

where x, y and z correspond to the streamwise, spanwise and vertical directions in a cartesian coordinate system. Here $\widetilde{\rho}$ and $\widetilde{T}$ are respectively defined as the instantaneous potential density and temperature of a fluid particle.

$$\widetilde{\rho}(x, y, z, t) \quad = \quad \rho - \rho_o - \rho_a(z) \quad = \quad \overline{\rho}(z) + \rho'(x, y, z, t) \tag{2.3}$$

$$\widetilde{T}(x, y, z, t) \quad = \quad T - T_o - T_a(z) \quad = \quad \overline{T}(z) + T'(x, y, z, t) \tag{2.4}$$

where ρ and T are the total density and temperature, ρ_o and T_o are the constant values for scaling density and temperature of the system, $\rho_a(z)$ and $T_a(z)$ are the adiabatic density and temperature variation when the fluid is adiabatically moved to reference pressure, $\overline{\rho}(z)$ and $\overline{T}(z)$ are the background density and temperature, and ρ' and T' are the deviation from background density and temperature.

Each particle is identified by its originating position (x_o, y_o, z_o) at $t_o = 0$. The independent variables in the Lagrangian frame are the initial position (x_o, y_o, z_o) and the current time t. Thus, $\boldsymbol{x}(x_o, y_o, z_o, t)$ is the position of a fluid particle at t. A fundamental relationship between Lagrangian and Eulerian frames of reference is then, $\boldsymbol{x}(x_o, y_o, z_o, t) \ = \ (x, y, z, t)$.

The significance of the potential temperature and density is that their gradients determine the stability of the flow, i.e., $\frac{d\widetilde{T}}{dz} > 0$ or $\frac{d\widetilde{\rho}}{dz} < 0$ is a stable flow

condition whereas $\frac{dT}{dz} > 0$ or $\frac{d\rho}{dz} < 0$ condition can be unstable, i.e., it can be either $\frac{d\widetilde{T}}{dz} < 0$ or $\frac{d\widetilde{\rho}}{dz} > 0$ because the density at a lower region can decrease as the pressure effect on density is removed and does not compress the fluid particle anymore. Since $\widetilde{\rho}$ decreases with height in stable condition and it is the variable that determines the static stability, the use of potential density is appropriate for ensuring a stable stratification after an adiabatic density distribution.

From the Stokes's assumption, the thermodynamics absolute pressure can be interpreted as the mean pressure or the mechanical pressure related to only translational energy. Thus, pressure can be decomposed into a hydrostatic and nonhydrostatic pressure [23].

$$p \quad = \quad P + p' \tag{2.5}$$

where P is the hydrostatic pressure and p' is the perturbation from hydrostatic pressure. The hydrostatic pressure is associated with the fluid in static equilibrium state and determined by the hydrostatic force balance,

$$\frac{dP}{dz} \quad = \quad -(\rho_o + \bar{\rho})g \tag{2.6}$$

which represents the balance between net pressure force in the vertical and gravitational force of fluid particle associated with fluid particle's density.

2.1.1   Equation of motion - Boussinesq approximation

The Boussinesq approximation was introduced and applied to fluid dynamics by Boussinesq [4], and Spiegel and Veronis [48] formally justified the Boussinesq

approximation by performing a scaling analysis of equations. The study for Boussinesq flow is reviewed by many papers such as Durran & Arakawa [11] and Bannon [2].

The main purpose of the Boussinesq approximation is retaining the effects of density (buoyancy) and linearizing the acceleration terms in Navier-Stokes equation by ignoring density variations except where they are coupled with gravity. This assumption is applicable under certain conditions which are (i) compressibility effects are small so density does not change due to pressure change but may change due to temperature change and (ii) the vertical scale of the flow (H) is much smaller than any length scale ℓ, hence, $\frac{\Delta \bar{\rho}}{\rho_o} = \epsilon \ll 1$ [27, 48].

The general equations for conservation of mass and momentum for fully compressible flow of a Newtonian fluid are,

$$\frac{1}{\rho} \frac{D\rho}{Dt} = -\nabla \cdot \boldsymbol{v} \tag{2.7}$$

$$\rho \frac{D\boldsymbol{v}}{Dt} = -\nabla p - \rho g + \nabla \left(2\mu e_{ij} - \frac{2}{3}\mu(\nabla \cdot \boldsymbol{v})\delta_{ij} \right) \tag{2.8}$$

where $e_{ij} = \frac{1}{2} \left(\frac{\partial u_i}{\partial x_j} + \frac{\partial u_j}{\partial x_i} \right)$ is a strain rate tensor

For the Boussinesq flow, Spiegel and Veronis [48] show that the divergence of velocity $(\nabla \cdot \boldsymbol{v})$ contains order of ϵ which is much less than 1, and this term can be assumed to be very small, approximately zero. From the conservation of mass,

$$\frac{1}{\rho} \frac{D\rho}{Dt} = -\nabla \cdot \boldsymbol{v} = -\left(\frac{\partial}{\partial t} + \boldsymbol{v} \cdot \nabla \right) \left(\epsilon \frac{\bar{\rho}}{\Delta \bar{\rho}} + \epsilon \frac{\rho'}{\Delta \bar{\rho}} \right) + \mathcal{O}(\epsilon^2) \approx 0 \tag{2.9}$$

In the Boussinesq approximation, the thermodynamic variables such as specific heats (c_p & c_v), volumetric expansion coefficient (α), and transport properties

such as thermal conductivity (k) and viscosity (μ) are assumed to be constant. The equation of state for Boussinesq flow gives,

$$\rho(T) \;=\; \rho_o[1 - \alpha(T - T_o)] \tag{2.10}$$

For an ideal gas, it obeys an equation of state which is given by,

$$p = \rho RT \tag{2.11}$$

where R is a specific gas constant

The change in internal energy is given by,

$$de \;=\; c_v dT \tag{2.12}$$

where e is a specific internal energy and c_v is a specific heat at constant volume

The mechanical energy for the Boussinesq flow is obtained by multiplying (2.8) $\boldsymbol{v}$ with Boussinesq approximation by which gives,

$$\rho_o \frac{D}{Dt}\left(\frac{1}{2}u_i^2 + gz\right) \;=\; \frac{\partial}{\partial x_j}(u_i \tau_{ij}) + p(\nabla \cdot \boldsymbol{v}) \tag{2.13}$$

where $\tau_{ij} = -p\delta_{ij} + 2\mu e_{ij}$ and $\frac{\partial}{\partial x_j}(u_i \tau_{ij}) = -p(\nabla \cdot \boldsymbol{v}) - \boldsymbol{v}(\nabla p) + \mu \nabla^2 \boldsymbol{v}$

The total energy equation for the Boussinesq flow is given by [27],

$$\rho_o \frac{D}{Dt}\left(e + \frac{1}{2}u_i^2 + gz\right) \;=\; \frac{\partial}{\partial x_j}(u_i \tau_{ij}) + \frac{\partial q_i}{\partial x_i} \tag{2.14}$$

The internal energy equation can be obtained by subtracting mechanical energy (2.13) from total energy (2.14).

$$\rho_o \frac{De}{Dt} \;=\; -\nabla \cdot \mathbf{q} - p(\nabla \cdot \boldsymbol{v}) \tag{2.15}$$

The internal energy equation combined with (2.4), (2.11) and (2.12) reduces to an equation for temperature.

$$
\begin{aligned}
\rho_o \frac{De}{Dt} &= -\nabla \cdot \mathbf{q} - p(\nabla \cdot \boldsymbol{v}) \\
\rho_o c_v \frac{DT}{Dt} &= -\nabla \cdot \mathbf{q} + \frac{p}{\rho} \frac{D\rho}{Dt} \\
\rho_o c_v \frac{DT}{Dt} &= -\nabla \cdot \mathbf{q} - (-\frac{Dp}{Dt} + \rho R \frac{DT}{Dt}) \\
\rho_o (c_v + R) \frac{DT}{Dt} &= -\nabla \cdot \mathbf{q} + \frac{Dp}{Dt} \\
\frac{DT}{Dt} &= \kappa \nabla^2 T \\
\frac{D\widetilde{T}}{Dt} &= \kappa \nabla^2 \widetilde{T}
\end{aligned}
\tag{2.16}
$$

where $\mathbf{q} = -k\nabla T$ is a heat flux obeying the Fourier law, k is the thermal conductivity, $\kappa = \frac{k}{\rho_o c_p}$ is the scalar thermal diffusivity, c_p is a specific heat at constant pressure, and $\frac{Dp}{Dt}$ is negligible under the Boussinesq approximation.

Combining (2.16) with (2.3) and (2.10) gives the density equation which has same form as temperature equation.

$$
\frac{D\widetilde{\rho}}{Dt} = \kappa \nabla^2 \widetilde{\rho}
\tag{2.17}
$$

(2.17) shows that the density changes due to thermal diffusion.

The momentum equation (2.8) for a fluid particle in the Boussinesq flow with $\nabla \cdot \boldsymbol{v} \approx 0$ condition is,

$$
\rho \frac{D\boldsymbol{v}}{Dt} = -\nabla p + \mu \nabla^2 \boldsymbol{v} - \rho g
\tag{2.18}
$$

Subtracting the hydrostatic balance of background (2.6) from (2.18) and dividing by ρ_o gives the conservation of momentum for the Boussinesq flow,

$$
\begin{aligned}
\rho \frac{D\boldsymbol{v}}{Dt} &= -\nabla p' + \mu \nabla^2 \boldsymbol{v} - \rho' g \\
\left(1 + \frac{\Delta \overline{\rho}}{\rho_o} + \frac{\rho'}{\rho_o}\right) \frac{D\boldsymbol{v}}{Dt} &= -\frac{1}{\rho_o} \nabla p' + \nu \nabla^2 \boldsymbol{v} - \frac{\rho'}{\rho_o} g \\
\frac{D\boldsymbol{v}}{Dt} &= -\frac{1}{\rho_o} \nabla p' + \mu \nabla^2 \boldsymbol{v} - \frac{\rho'}{\rho_o} g
\end{aligned}
\tag{2.19}
$$

In summary, from (2.9), (2.19) and (2.17), the equations of motion for a fluid particle in a uniformly stratified flow with the Boussinesq approximation are:

$$
\nabla \cdot \boldsymbol{v} \approx 0
\tag{2.20}
$$

$$
\frac{D\boldsymbol{v}}{Dt} = -\frac{1}{\rho_o} \nabla p' + \nu \nabla^2 \boldsymbol{v} - \frac{\rho'}{\rho_o} g
\tag{2.21}
$$

$$
\frac{D\widetilde{\rho}}{Dt} = \frac{\partial \widetilde{\rho}}{\partial t} + \boldsymbol{v} \cdot \nabla \widetilde{\rho} = \kappa \nabla^2 \widetilde{\rho}
\tag{2.22}
$$

In Bousinessq flow with molecular (thermal) diffusion and ideal gas behavior, the equation for internal energy (2.16) is converted to an equation for density, which as shown in chapter 3, will be considered in terms of potential energy. Therefore, in this study, we will focus only on the mechanical energy components, kinetic energy and potential energy. Alternatively, if the conversion is made back from $\widetilde{\rho}$ to $\widetilde{T}$, changes in the (diabatic) component of potential energy would be considered as changes in internal energy.

Chapter 3

Lagrangian Energetics

In this chapter, we develop a Lagrangian analysis of the energetics of stably stratified Boussinesq flow with a particular focus on the description of potential energy. The total potential energy of a fluid particle is considered as the sum of the available potential energy (associated with nonequilibrium displacement) and reference potential energy (associated with the change in particle equilibrium level). The use of PE components in the Lagrangian frame has several advantages: they are sign-positive definite, independent of the coordinate system, and can be directly related to the square of vertical displacement in uniform stratified flows [28]. The associated evolution equations will indicate the key underlying physics. The developed analysis will then be applied to the problem of homogeneous turbulent dispersion in chapter 4. Results will give an expression for the behavior of mean square vertical displacement and clarify the role of mixing.

We first briefly examine potential energy (PE) components in the Eulerian

framework and then develop PE components in the Lagrangian framework in the following section. We will then compare these two analyses. Finally, application to a uniform stratified turbulence is considered and the corresponding evolution equations for the PE components in the Lagrangian frame are developed.

3.1 Potential Energy Analysis - Eulerian Framework

As discussed in chapter 1, the energetics of stratified flow is usually formulated in the Eulerian framework which considers a region of space, i.e., a control volume, for analysis. The total potential energy (TPE) is described as the sum of available potential energy (APE) and background potential energy (BPE).

3.1.1 Total Potential Energy

The potential energy (per unit volume) at a given z location may be evaluated as $\rho g z$, where ρ is the density of the fluid and z is a vertical height defined with respect to an arbitrary datum. In the Eulerian energetics developed by Winters et al. [68], the total potential energy (TPE) for the domain (control volume) is then

$$E_p \quad = \quad g \int \rho z \, dV \tag{3.1}$$

3.1.2   Background and Available Potential Energy

Lorenz [31] defined the reference state as the minimum energy state and no further conversion occurs between PE and KE, i.e., the reference state is an undisturbed stable ($\frac{d\rho}{dz} < 0$) state in hydrostatic equilibrium ($\boldsymbol{v} = 0$). The corresponding PE of this reference state is BPE (Background Potential Energy) and is used to define APE from TPE. Winters et al. [68] defined BPE as the minimum potential energy for a given volume and time and obtained through an adiabatic redistribution of the actual density, ρ, to give $\rho(z_{*1}) > \rho(z_{*2})$ when $z_{*1} < z_{*2}$ so that the resulting density distribution is a decreasing function of z_* [66]. The BPE is then given by,

$$
\begin{aligned}
E_b &= g \int z_*(\boldsymbol{x}, t)\rho(\boldsymbol{x}, t)\, dV \\
&= gA \int \rho(z_*, t)z_*\, dz_*
\end{aligned}
\tag{3.2}
$$

where $z_*(\boldsymbol{x}, t)$ is the corresponding vertical position of fluid in the reference state of fluid at $(\boldsymbol{x}, t)$ in the actual state.

The APE is then obtained by subtracting BPE (3.2) from TPE (3.1),

$$
E_a = g \int \rho(z - z_*)\, dV
\tag{3.3}
$$

As discussed in chapter 1, the APE is the portion of TPE available for conversion to kinetic energy (KE).
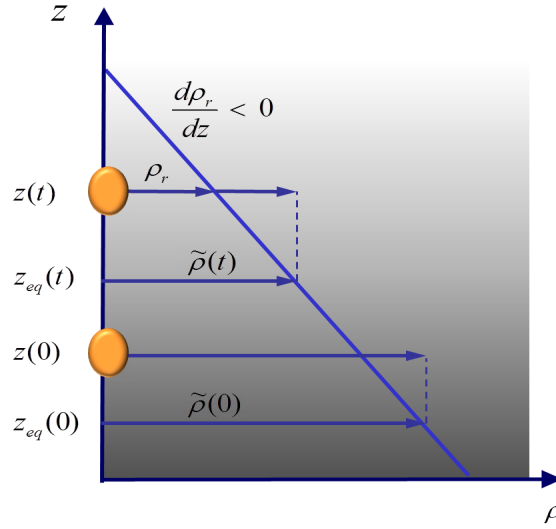
Figure 3.1: Diagram of a fluid particle's reference density and height. In this case shown, the reference density variation $\rho_r(z)$ is linear.

3.2 Lagrangian analysis

For the development of PE components in Lagrangian framework, the Lagrangian variables first need to be established. The PE (per unit volume) of a fluid particle, which resides at a height z at time t could be evaluated as

$$\widetilde{\rho}(t)gz(t) \tag{3.4}$$

where a natural datum for z would be the initial position $z(0)$. However, as will be shown, in considering the energetics and the partitioning of PE, we will consider $z_{eq}(0)$ for the datum, so that the particle vertical position can be written as

$$
\begin{aligned}
z_p(t) &= z(t) - z_{eq}(0) \\
&= (z(t) - z_{eq}(t) + (z_{eq}(t) - z_{eq}(0)) \\
&= z'(t) + \Delta z_{eq}(t)
\end{aligned}
\tag{3.5}
$$

where z_p is the total vertical particle displacement, defined with respect to its *original equilibrium reference height* $z_{eq}(0)$. The equilibrium reference height is the height where the density of fluid particle $\widetilde{\rho}(t)$ equals the reference density $\rho_r(z)$, which is the redistributed density field obtained from an adiabatic rearrangement such that $\rho_r(z_1) > \rho_r(z_2)$ when $z_1 < z_2$.

Figure 3.1 illustrates the decomposition of the fluid particle's vertical position and corresponding density. We consider a fluid particle with an initial position $z(0)$ and initial density $\widetilde{\rho}(0)$. $z_{eq}(t)$ is the equilibrium reference height of a particle whose density $\widetilde{\rho}(t)$ matches the reference density $\rho_r(z)$. $z_{eq}(0)$ is the original equilibrium reference height at $t = 0$ and Δz_{eq} is the change in the particle's equilibrium reference height. z' is the deviation of the particle's current height $z(t)$ from the particle's current equilibrium reference height. With these defined Lagrangian variables, we will develop the potential energy components in Lagrangian framework.

3.2.1 Available Potential Energy Density

The locally defined APE density (hereafter denoted as $\mathcal{E}_{ap}$) in the Lagrangian framework was proposed by Holliday and McIntyre [14] for an adiabatic process, i.e., there is no molecular diffusion and thus the density of a fluid particle remains constant in this case. APE density is associated with the difference between the actual density, $\widetilde{\rho}(t) = \widetilde{\rho}(0)$, and reference density, $\rho_r(z)$ [54] and defined

as,

$$
\begin{aligned}
\mathcal{E}_{ap} &= \int_{z_{eq}(0)}^{z(t)} g(\widetilde{\rho}(0) - \rho_r(\hat{z}))\, d\hat{z} \\
&= \widetilde{\rho}(0)g(z(t) - z_{eq}(0)) - \int_{z_{eq}(0)}^{z(t)} g\rho_r(\hat{z})\, d\hat{z} \\
&= \widetilde{\rho}(0)g(z(t) - z_{eq}(0)) + P(z(t)) - P(z_{eq}(0)) \qquad (3.6)
\end{aligned}
$$

where $z_{eq}(0)$ is the (constant) equilibrium height, $\hat{z}$ is the dummy variable of integration, and $P(z(t))$ and $P(z_{eq}(0))$ are the hydrostatic pressures at $z(t)$ and $z_{eq}(0)$ respectively

Based on (3.6), the interpretation of $\mathcal{E}_{ap}$ is the amount of energy required for a fluid particle with density $\widetilde{\rho}(0)$ to move from its equilibrium height ($z_{eq}(0)$) to a new height, $z(t)$. The amount of work of $\widetilde{\rho}(0)g(z - z_{eq}(0))$ is needed to overcome the gravitational force in figure 3.1. However, all of this work is not required to move a fluid particle from $z_{eq}(0)$ to $z(t)$ because of the favorable pressure gradient which is is associated with an inactive portion of PE and is responsible for equilibrium [23]. Therefore, (3.6) represents the net energy required for a fluid particle to move from $z_{eq}(0)$ to $z(t)$ which is also the amount of PE energy available for conversion to KE.

The above definition of APE density (3.6) was extended by Roullet and Klein [44] and Molemaker and McWilliams [33] to include diabatic effects. The constant equilibrium height ($z_{eq}(0)$) and density ($\widetilde{\rho}(0)$) are replaced by an instanta-

neous equilibrium height $(z_{eq}(t))$ and instantaneous density of fluid particle $(\widetilde{\rho}(t))$,

$$
\begin{aligned}
\mathcal{E}_{ap} &= \int_{z_{eq}(t)}^{z(t)} g(\widetilde{\rho}(t) - \rho_r(\hat{z}))\, d\hat{z} \\
&= g\int_{z_{eq}(t)}^{z(t)} \widetilde{\rho}(t)\, d\hat{z} \;-\; g\int_{z_{eq}(t)}^{z(t)} \rho_r(\hat{z})\, d\hat{z}
\end{aligned}
\tag{3.7}
$$

Recall that the full description of PE in the Eulerian framework consists of two components, APE and BPE. We have now considered corresponding APE and analogous with the Eulerian framework, we need to define an additional energy quantity which is consistent with BPE in Eulerian analysis.

3.2.2 Reference Potential Energy Density

The PE of a fluid particle is defined $w.r.t.$ the particle vertical displacement (3.5). APE is defined $w.r.t.$ the displacement from $z_{eq}(t)$ to $z(t)$, we now consider the energy associated with the remaining portion of z_p, i.e., from $z_{eq}(0)$ to $z_{eq}(t)$.

The minimum energy to change the fluid particle's reference state in Lagrangian framework can be determined by evaluating the difference between the initial *reference density* and the instantaneous *reference density* as the corresponding reference height of fluid particles changes from $z_{eq}(0)$ to $z_{eq}(t)$. We consider the RPE (Reference Potential Energy) to be the energy required to change the reference state of fluid particles. We can define the RPE density consistent with the APE density as the minimum energy required to elevate a fluid particle with $\widetilde{\rho}(0)(= \rho_r(z_{eq}(0)))$ at $z_{eq}(0)$ from its initial reference state $(z_{eq}(0))$ to a new reference state $(z_{eq}(t))$ in figure 3.1. We define the RPE density (hereafter denoted as

$\mathcal{E}_{rp}$)

$$\begin{aligned}
\mathcal{E}_{rp} &= \int_{z_{eq}(0)}^{z_{eq}(t)} g(\rho_r(z_{eq}(0)) - \rho_r(\hat{z}(t)))\, d\hat{z} \\
&= \int_{z_{eq}(0)}^{z_{eq}(t)} g(\widetilde{\rho}(0) - \rho_r(\hat{z}))\, d\hat{z} \\
&= g \int_{z_{eq}(0)}^{z_{eq}(t)} \widetilde{\rho}(0)\, d\hat{z} - g \int_{z_{eq}(0)}^{z_{eq}(t)} \rho_r(\hat{z})\, d\hat{z} \qquad (3.8)
\end{aligned}$$

In (3.8), RPE depends only on reference density, the actual state which can be changed only by molecular diffusion, and independent of current height. RPE is non-available energy because the new thermodynamic equilibrium reference state cannot return to its initial reference state without heat transfer, due to irreversible mixing. As will be shown (see figure 3.2), $\mathcal{E}_{rp}$ is a positive definite quantity which is independent of the particle's direction of movement.

3.2.3   Total Potential Energy in Lagrangian analysis

Both the potential energy components, APE and RPE density, are now defined and TPE density (hereafter represented as $\mathcal{E}_{tp}$) is expressed as the sum of APE and RPE density.

$$\mathcal{E}_{tp} = \underbrace{\int_{z_{eq}(t)}^{z(t)} g(\widetilde{\rho}(t) - \rho_r(\hat{z}))\, d\hat{z}}_{Available\ PE} + \underbrace{\int_{z_{eq}(0)}^{z_{eq}(t)} g(\rho_r(z_{eq}(0)) - \rho_r(\hat{z}))\, d\hat{z}}_{Reference\ PE} \qquad (3.9)$$

3.3 Eulerian and Lagrangian framework comparison

In this section, we will compare the PE components in the Lagrangian and Eulerian framework for a closed system with a uniform stratification, in which case the Eulerian system (finite volume) will be the same as the Lagrangian system (an ensemble of fluid particles).

3.3.1 Ensemble average of PE in Lagrangian framework

The APE density in (3.7) represents one fluid particle's APE and the ensemble average of all the fluid particles' APE density gives a total APE per unit volume denoted by E_{ap},

$$
\begin{aligned}
E_{ap} &= \frac{\sum\limits_{N=1}^{N} \left(\int_{z_{eq}(t)}^{z(t)} g(\widetilde{\rho}(t) - \rho_r(\hat{z})) \, d\hat{z} \right)}{N} \\
&= \left\langle g \int_{z_{eq}(t)}^{z(t)} \widetilde{\rho}(t) \, d\hat{z} \right\rangle - \left\langle g \int_{z_{eq}(t)}^{z(t)} \rho_r(\hat{z}) \, d\hat{z} \right\rangle \quad (3.10) \\
&= g\langle z'\widetilde{\rho}(t) \rangle \quad (3.11)
\end{aligned}
$$

where $N =$ total number of fluid particles, $\frac{1}{N} \sum\limits_{N=1}^{N}$ is ensemble average denoted by $\langle \ \rangle$ and the ensemble average of second term in (3.10) vanishes because when the fluid particles exchange their position for a closed system, they have same amount of pressure gradient force but opposite sign as shown by Winters and Barkan [66].

Similarly, the RPE density in (3.6) represents one fluid particle's RPE and the total RPE denoted by E_{rp} is obtained by taking an ensemble average over all

the fluid particles. Total RPE per unit volume of all the fluid particles is given by

$$
\begin{aligned}
E_{rp} &= \frac{\sum_{N=1}^{N}\left(\int_{z_{eq}(0)}^{z_{eq}(t)} g(\widetilde{\rho}(0) - \rho_r(\hat{z}))\,d\hat{z}\right)}{N} \\
&= \frac{\sum_{N=1}^{N}\left(g\Delta z_{eq}\widetilde{\rho}(0) - g\int_{z_{eq}(0)}^{z_{eq}(t)} \rho_r(\hat{z})\,d\hat{z}\right)}{N} \\
&= g\langle\Delta z_{eq}\widetilde{\rho}(0)\rangle - \left\langle g\int_{z_{eq}(0)}^{z_{eq}(t)} \rho_r(\hat{z})\,d\hat{z}\right\rangle \\
&= g\langle\Delta z_{eq}\widetilde{\rho}(0)\rangle
\end{aligned}
\tag{3.12}
$$

where $\left\langle g\int_{z_{eq}(0)}^{z_{eq}(t)} \rho_r(\hat{z})\,d\hat{z}\right\rangle$, the work done by the pressure gradient force of all the fluid particles, is zero since all of the fluid particles switch their positions for a closed system [66].

From (3.11) and (3.12), TPE per unit volume of all the fluid particles denoted by E_{tp} is given by

$$
E_{tp} = g\langle z'\widetilde{\rho}(t)\rangle + g\langle\Delta z_{eq}\widetilde{\rho}(0)\rangle
\tag{3.13}
$$

3.3.2 Available Potential Energy comparison

Andrews [1] showed that the volume-integrated APE density is in general greater than or equal to Lorenz's APE ($\int_V E_{ap}\,dV \geq APE_{Lorenz}$). However, if the reference state in APE density equals Lorenz's reference state, the volume-integrated APE density equals Lorenz's APE [1, 54].

$$
\begin{aligned}
\frac{E_a}{V} &= \frac{g\int \rho(z - z_*)\,dV}{V} \\
&= g\overline{\rho(z - z_*)}, \quad \text{spatial average}
\end{aligned}
\tag{3.14}
$$

where V is the total volume of a domain.

The equation (3.11) and (3.14) show that E_{ap} in Lagrangian framework is equal to APE_{Lorenz} per unit volume in Eulerian framework, i.e., $\overline{g\rho(x,t)(z-z_*)} = g\langle z'\widetilde{\rho}(t)\rangle$ because the volume average is equal to the ensemble average of all fluid particles in a given volume.

3.3.3 Non-available Potential Energy comparison

In the $\rho - z_*$ coordinate system of Eulerian framework, the minimum energy to change the reference state (ΔE_b) is determined by evaluating the density change $(\Delta\rho = \rho(t,z_*) - \rho(0,z_*))$ at fixed position $(z_*(0,\rho))$ and integrating over z_*.

$$
\begin{aligned}
\Delta E_b &= gA\int \rho(t,z_*)z_* \, dz_* - gA\int \rho(0,z_*)z_* \, dz_* \\
&= gA\int \Delta\rho z_* \, dz_*
\end{aligned}
\tag{3.15}
$$

Equation (3.15) represents the minimum energy required to change the density due to mixing over the volume. From (3.15), the change of BPE per unit volume is given by,

$$
\begin{aligned}
\frac{\Delta E_b}{V} &= \frac{gA\int_{z_{*,bottom}}^{z_{*,top}} \Delta\rho z_* \, dz_*}{A(z_{*,top} - z_{*,bottom})} \\
&= g\overline{\Delta\rho z_*(0,\rho)}, \quad \text{spatial average} \tag{3.16} \\
&= g\overline{\left(\frac{d\rho}{dz_*}\right)\Delta z_* \left(\frac{dz_*}{d\rho}\right)\rho} \\
&= g\overline{\Delta z_*\rho(0,z_*)} \tag{3.17}
\end{aligned}
$$

(a) RPE density in Lagrangian framework   (b) ΔE_b density in Eulerian framework
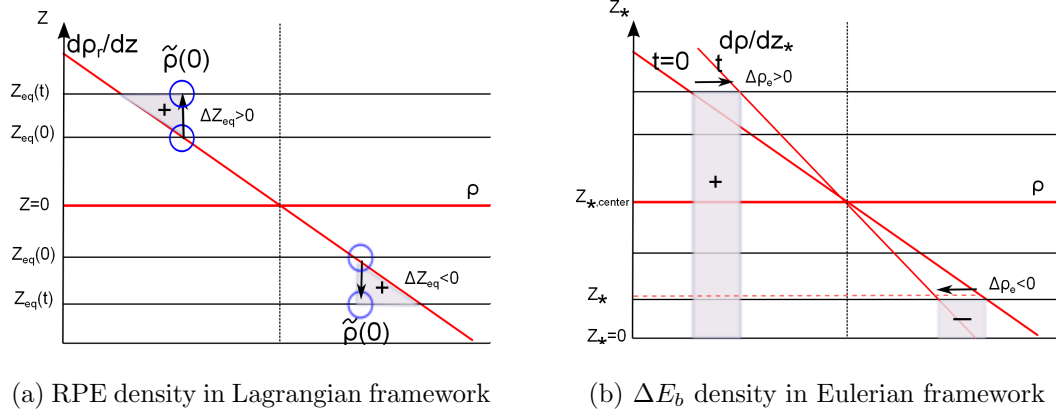
Figure 3.2: RPE density and ΔE_b density comparison

where $V = -A(z_{*,bottom} - z_{*,top})$, $z_{*,bottom}$ and $z_{*,top}$ are the reference position at the bottom and top of the control volume respectively and $\Delta z_* = z_*(t, \rho(t)) - z_*(0, \rho(t))$ is the difference between the initial and instantaneous reference position equivalent to the change in reference height (Δz_{eq}) in the Lagrangian framework.

Therefore, from (3.12) and (3.17), RPE per unit volume equals to ΔE_b per unit volume for the same initial density profile, i.e., the initial reference density of flow $(\rho(z_*(0)))$ in Eulerian framework is equal to the initial density of fluid parti-cles $(\widetilde{\rho}(z(0)))$ in Lagrangian framework. $g\overline{\Delta z_* \rho(0, z_*)} = g\langle \Delta z_{eq} \widetilde{\rho}(0) \rangle$ because the volume average is equal to the ensemble average of all particles for a homogeneous fluid in a closed system. From (3.12) and (3.16), the effect of mixing on change in reference density in Eulerian framework is equivalent to the effect of mixing on change in reference height in Lagrangian framework and both thereby represent the change in reference state.

The RPE density in (3.8) is always positive for any fluid particle moving

above or below the centerline ($z = \frac{L}{2}$, $L =$ domain length) as it is illustrated in figure 3.2a which shows positive triangle area in both directions. When a fluid particle moves up, the density of fluid particle $\widetilde{\rho}(0)$ is greater than reference density $\rho_r(z)$ and change in equilibrium level Δz_{eq} is positive. Since $\widetilde{\rho}(0) - \rho_r(z)$ and Δz_{eq} are both positive, $\mathcal{E}_{rp}$ has a positive value from (3.8). When the fluid particle moves down, the density of fluid particle $\widetilde{\rho}(0)$ is smaller than reference density $\rho_r(z)$ and change in equilibrium level Δz_{eq} is negative. Since $\widetilde{\rho}(0) - \rho_r(z)$ and Δz_{eq} are both negative, $\mathcal{E}_{rp}$ has a positive value from (3.8). The arrows in figure 3.2a represents the density change of fluid particles which is equivalent to the change in reference density profile in figure 3.2b. In comparison, ΔE_b density can be positive or negative in figure 3.2b, even though the volume average of ΔE_b is always positive. The ΔE_b density equation in (3.17) shows a positive value above the centerline in z_* coordinate and negative value below the centerline as it is illustrated in figure 3.2b. RPE density which is positive definite is not the same as ΔE_b density but total RPE is equal to total ΔE_b.

In summary, the change in background potential energy (ΔE_b) is the difference between the instantaneous and initial reference density profile. RPE corresponds to the difference between instantaneous and the initial equilibrium level associated with the density of fluid particle with a given initial reference density. The density change of all fluid particles in Lagrangian framework is equivalent to the change in reference density profile in Eulerian framework. Finally, if the initial reference density profile is same, Lagrangian and Eulerian frame can be considered

equivalent for a closed system.

3.4   Application to uniform stratified turbulence

We now consider the particular case of an unbounded homogeneous turbulent flow with uniform background stable stratification ($d\overline{\rho}/dz = \text{constant} < 0$). In this case, the background density corresponds to the mean (spatial average) density which only varies in the vertical direction, i.e., $\overline{\rho} = \overline{\rho}(z)$. The instantaneous potential density and temperature of a fluid particle are also decomposed into a mean part and a fluctuating part.

$$\widetilde{\rho}(x, y, z, t) \;\; = \;\; \widehat{\rho}(z) + \rho''(x, y, z, t) \tag{3.18}$$

$$\widetilde{T}(x, y, z, t) \;\; = \;\; \widehat{T}(z) + T''(x, y, z, t) \tag{3.19}$$

where $\widehat{\rho}(z)$ and $\widehat{T}(z)$ are a horizontally homogeneous mean (ensemble average) density and temperature depending only on vertical position, and ρ'' and T'' are the fluctuation of the potential density of fluid particle from the mean density and the fluctuation of the potential temperature of fluid particle from the mean temperature. In this study, the deviation from the background density ρ' is equal to the fluctuation from the mean density ρ'' and the background density is equal to mean density, i.e., $\rho' = \rho''$ and $\overline{\rho}(z) = \widehat{\rho}(z)$. From here on, we will use prime ($'$) to indicate fluctuations from mean values.

The instantaneous velocity is decomposed into a mean part ($\overline{U}$) and a fluc-

tuating part ($\boldsymbol{v}'$).

$$\boldsymbol{v}(x,y,z,t) = \overline{U}(z) + \boldsymbol{v}'(x,y,z,t) \tag{3.20}$$

where $\overline{U}(z)$ is the mean x-component (horizontal) velocity which can vary in z, i.e., vertical mean shear may exist.

In the case of uniform stably stratified flow ($\frac{d\overline{\rho}}{dz} = $ constant), the reference density, $\rho_r(z)$, is replaced by the horizonal average density, $\overline{\rho}(z)$, which is equal to Lorenz's adiabatically rearranged reference density state. The APE density equation then is

$$\mathcal{E}_{ap} = g \int_{z_{eq}(t)}^{z(t)} (\widetilde{\rho}(t) - \overline{\rho}(\hat{z}))\, d\hat{z} \tag{3.21}$$

and from (3.8), RPE density equation is,

$$\mathcal{E}_{rp} = g \int_{z_{eq}(0)}^{z_{eq}(t)} (\widetilde{\rho}(0) - \overline{\rho}(\hat{z}))\, d\hat{z} \tag{3.22}$$

Equation (3.21) and (3.22) will be applied to develop the model for mean square vertical displacement in a uniform stably stratified flow in chapter 4.

3.5   Evolution of Energetics

The potential energy quantities have been defined. The evolution equations of these quantities need to be developed to examine the underlying physical processes and associated energy conversion.

3.5.1 Evolution of density

The density of a fluid particle evolves according to (2.22):

$$\frac{D\widetilde{\rho}}{Dt} = \kappa\nabla^2\widetilde{\rho} \tag{2.22}$$

The material derivative of the mean density $(\overline{\rho}(z))$ of a fluid particle is expressed by,

$$\frac{D\overline{\rho}}{Dt} = \frac{\partial\overline{\rho}}{\partial t} + w'\frac{\partial\overline{\rho}}{\partial z} = w'\frac{\partial\overline{\rho}}{\partial z} \tag{3.23}$$

Subtracting (3.23) from (2.22) yields the evolution equation for the density fluctuation ρ',

$$\frac{D\rho'}{Dt} = -w'\frac{d\overline{\rho}}{dz} + \kappa\nabla^2\widetilde{\rho} . \tag{3.24}$$

The equation indicates that changes in ρ' are due to changes in $\overline{\rho}(z)$ by vertical advection w' and changes in particle density by molecular diffusion.

Integrating (3.24) with respect to time,

$$
\begin{aligned}
\rho'(t) - \rho'(0) &= (z(t) - z(0))\left(-\frac{d\overline{\rho}}{dz}\right) + \int_0^t \kappa\nabla^2\widetilde{\rho}\,d\tau \\
&= -(\overline{\rho}(z(t)) - \overline{\rho}(0)) + \Delta\widetilde{\rho} .
\end{aligned}
\tag{3.25}
$$

The vertical displacement of a fluid particle from its initial position is given by

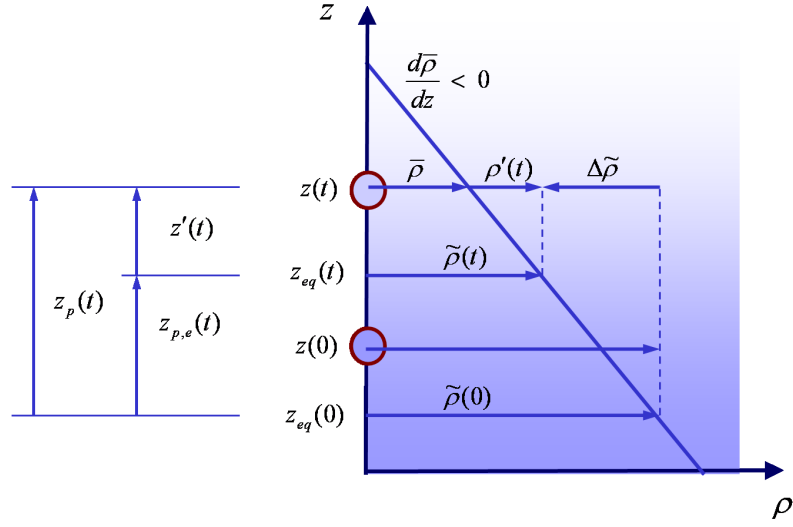$$\Delta z = z(t) - z(0) = \int_0^t w'\,d\tau . \tag{3.26}$$

Figure 3.3: Diagram of fluid particle density and displacement decompositions.

From (3.25), Δz may also be expressed as,

$$
\begin{aligned}
z(t) - z(0) &= \frac{\rho'(t)}{-d\overline{\rho}/dz} - \frac{\rho'(0)}{-d\overline{\rho}/dz} + \frac{\Delta\widetilde{\rho}}{d\overline{\rho}/dz} \\
&= (z(t) - z_{eq}(t)) - (z(0) - z_{eq}(0)) + (z_{eq}(t) - z_{eq}(0)) \quad (3.27)
\end{aligned}
$$

From this, we redefine the particle displacement to be (as indicated in (3.5)),

$$
\begin{aligned}
z(t) - z_{eq}(0) &= (z(t) - z_{eq}(t)) + (z_{eq}(t) - z_{eq}(0)) \\
z_p(t) &= z'(t) + \Delta z_{eq}(t) \quad (3.28)
\end{aligned}
$$

where z' is the deviation from the particle's current equilibrium reference height, i.e., the nonequilibrium displacement, and Δz_{eq} is the change in the particle's equilibrium reference height, i.e., the equilibrium displacement. A diagram illustrating the displacements and corresponding densities is given in Figure 3.3.

VS [62] considered the vertical displacement in terms of an adiabatic displacement and a diabatic displacement which correspond to the two components in (3.28), the nonequilibrium displacement, z', and the change in particle equilibrium level, Δz_{eq}, respectively. The time derivative of the vertical displacement of a fluid particle in (3.28) gives the decomposition of the vertical velocity components, adiabatic velocity and diabatic velocity, as done by VS [62] in their analysis:

$$\frac{Dz_p}{Dt} \quad = \quad \frac{Dz'}{Dt} \quad + \quad \frac{Dz_{eq}}{Dt} \tag{3.29}$$

where $\frac{Dz_p}{Dt}$ is a total vertical velocity, $\frac{Dz'}{Dt}$ is an adiabatic vertical velocity, and $\frac{Dz_{eq}}{Dt}$ is a diabatic vertical velocity.

3.5.2 Evolution of Turbulent Kinetic Energy

From (2.21), the time development of the components of the fluid particle kinetic energy (per unit volume) with an uniform mean vertical shear is obtained,

$$\rho_o \frac{D\frac{1}{2}u'^2}{Dt} \quad = \quad - \rho_o u' w' \frac{d\overline{U}}{dz} - u' \frac{\partial p'}{\partial x} + \mu \, u' \nabla^2 u' \tag{3.30}$$

$$\rho_o \frac{D\frac{1}{2}v'^2}{Dt} \quad = \quad - v' \frac{\partial p'}{\partial y} + \mu \, v' \nabla^2 v' \tag{3.31}$$

$$\rho_o \frac{D\frac{1}{2}w'^2}{Dt} \quad = \quad - w' \frac{\partial p'}{\partial z} + \mu \, w' \nabla^2 w' - g \rho' w' \tag{3.32}$$

Taking an ensemble average over all particles and assuming homogeneous flow and negligible diffusion of kinetic energy with high Re, the evolution equation for the ensemble mean turbulent kinetic energy (TKE), $E_k = \rho_o \langle u'^2 + v'^2 + w'^2 \rangle / 2$,

$$\frac{DE_k}{Dt} \quad = \quad - \rho_o \langle u'w' \rangle \frac{d\overline{U}}{dz} - \varepsilon_k - g \langle \rho'w' \rangle \tag{3.33}$$

where ε_k is the total dissipation rate of TKE

3.5.3 Evolution of Available Potential Energy

From (3.21), the evolution equation of APE density in the Lagrangian frame is derived as

$$
\begin{aligned}
\frac{D\mathcal{E}_{ap}}{Dt} &= \frac{D}{Dt} \int_{z_{eq}(t)}^{z(t)} g(\widetilde{\rho}(t) - \rho_r(\hat{z}))\, d\hat{z} \\
&= g\left(z' \frac{D\widetilde{\rho}(t)}{Dt} + \widetilde{\rho}(t) \frac{Dz'}{Dt} \right) \\
&\quad - g\left(\rho_r(z) \frac{Dz}{Dt} - \rho_r(z_{eq}) \frac{Dz_{eq}}{Dt} \right) - \int_{z_{eq}(t)}^{z(t)} g \frac{\partial \rho_r}{\partial t}\, d\hat{z}
\end{aligned}
$$

where the reference density of the flow in Lagrangian framework is fixed in time, $\frac{\partial \rho_r}{\partial t} = \frac{\partial \overline{\rho}}{\partial t} = 0$, and for the uniform stratified flow, $\rho_r(z) = \overline{\rho}(z)$, $\rho_r(z_{eq}(t)) = \widetilde{\rho}(t)$.

Therefore, the evolution equation of APE density is given by

$$
\begin{aligned}
\frac{D\mathcal{E}_{ap}}{Dt} &= g(\widetilde{\rho} - \overline{\rho})w' + gz' \frac{D\widetilde{\rho}(t)}{Dt} \\
&= g\rho'w' - \frac{\kappa g}{d\overline{\rho}/dz} \rho' \nabla^2 \widetilde{\rho} \\
&= g\rho'w' - \left(-\frac{\kappa g}{d\overline{\rho}/dz}(\nabla\rho')^2 + \frac{\kappa g}{d\overline{\rho}/dz} \nabla^2\left(\frac{\rho'^2}{2}\right) \right) \quad (3.34)
\end{aligned}
$$

where $g\rho'w'$ is the buoyancy flux which is a reversible conversion from KE to APE from (3.32) and (3.34), $-\frac{\kappa g}{d\overline{\rho}/dz}(\nabla\rho')^2$ is the dissipation rate of APE, and $\frac{\kappa g}{d\overline{\rho}/dz}\nabla^2\left(\frac{\rho'^2}{2}\right)$ is the diffusion of APE.

The ensemble average of (3.34) gives the evolution equation of total APE.

$$
\begin{aligned}
\frac{DE_{ap}}{Dt} &= \langle g\rho'w'\rangle - \frac{\kappa g}{d\overline{\rho}/dz}\langle \rho'\nabla^2\widetilde{\rho}\rangle \\
&= B - \varepsilon_p - \frac{\kappa g}{d\overline{\rho}/dz}\left\langle \nabla^2\left(\frac{\rho'^2}{2}\right)\right\rangle \quad (3.35) \\
&= B - g\left(-\frac{d\overline{\rho}}{dz}\right)\varepsilon_\rho - \frac{\kappa g}{d\overline{\rho}/dz}\left\langle \nabla^2\left(\frac{\rho'^2}{2}\right)\right\rangle \quad (3.36)
\end{aligned}
$$

where B is the total buoyancy flux which is a reversible conversion from KE to

APE, $\varepsilon_p = -\frac{\kappa g}{d\overline{\rho}/dz}\langle(\nabla\rho')^2\rangle = g\left(-\frac{d\overline{\rho}}{dz}\right)\varepsilon_\rho$ is the total dissipation rate of APE, and

$\varepsilon_\rho = -\langle\kappa\nabla\rho'\cdot\nabla\rho'\rangle$.

3.5.4 Evolution of Reference Potential Energy

From (3.8), the evolution equation for RPE density in the Lagrangian frame

is given by

$$
\begin{aligned}
\frac{D\mathcal{E}_{rp}}{Dt} &= \frac{D}{Dt}\int_{z_{eq}(0)}^{z_{eq}(t)} g(\widetilde{\rho}(0) - \rho_r(\hat{z}))\,d\hat{z} \\
&= g\widetilde{\rho}(0)\frac{Dz_{eq}(t)}{Dt} \\
&\quad - g\left(\rho_r(z_{eq}(t))\frac{Dz_{eq}(t)}{Dt} - \rho_r(z_{eq}(0))\frac{Dz_{eq}(0)}{Dt} + \int_{z_{eq}(0)}^{z_{eq}(t)}\frac{\partial\rho_r}{\partial t}\,d\hat{z}\right)
\end{aligned}
$$

where $\rho_r(z_{eq}(t)) = \widetilde{\rho}(t)$, $\rho_r(z_{eq}(0)) = \widetilde{\rho}(0)$ and $\frac{\partial\rho_r}{\partial t} = \frac{\partial\overline{\rho}}{\partial t} = 0$

Therefore, the evolution equation of RPE density is given by

$$
\begin{aligned}
\frac{D\mathcal{E}_{rp}}{Dt} &= g\frac{Dz_{eq}}{Dt}(\widetilde{\rho}(0) - \widetilde{\rho}(t)) \\
&= \frac{\kappa g}{-d\overline{\rho}/dz}\Delta\widetilde{\rho}\nabla^2\widetilde{\rho} \quad (3.37)
\end{aligned}
$$

where $\frac{\kappa g}{-d\overline{\rho}/dz}\Delta\widetilde{\rho}\nabla^2\widetilde{\rho}$ is defined as the equilibrium mixing rate since it is associated

with the change in equilibrium state due to mixing.

Taking an ensemble average of (3.37) gives,

$$\frac{DE_{rp}}{Dt} = \frac{\kappa g}{-d\overline{\rho}/dz}\langle\Delta\widetilde{\rho}\nabla^2\widetilde{\rho}\rangle$$

$$= \Phi_m \qquad (3.38)$$

where $\Phi_m = \frac{\kappa g}{-d\overline{\rho}/dz}\langle\Delta\widetilde{\rho}\nabla^2\widetilde{\rho}\rangle$ is the total equilibrium mixing rate

From (3.29), the evolution of RPE can be written in terms of a diabatic velocity component.

$$\frac{DE_{rp}}{Dt} = \left\langle -g\Delta\widetilde{\rho}\frac{Dz_{eq}}{Dt}\right\rangle \qquad (3.39)$$

$$= \left\langle -g\Delta\widetilde{\rho}\left(\frac{Dz_p}{Dt} - \frac{Dz'}{Dt}\right)\right\rangle$$

$$= \langle -g\Delta\widetilde{\rho}w'\rangle + \frac{\kappa g}{d\overline{\rho}/dz}\langle\rho'\nabla^2\widetilde{\rho}\rangle + g\left(\frac{d\overline{\rho}}{dz}\right)\frac{D}{Dt}\langle\Delta z_{eq}z'\rangle$$

$$= \langle -g\Delta\widetilde{\rho}w'\rangle$$

$$+ \varepsilon_p + \frac{\kappa g}{d\overline{\rho}/dz}\left\langle\nabla^2\left(\frac{\rho'^2}{2}\right)\right\rangle + g\left(\frac{d\overline{\rho}}{dz}\right)\frac{D}{Dt}\langle\Delta z_{eq}z'\rangle \qquad (3.40)$$

The first term on the RHS of (3.40) may be negligible since the change in the fluid particle's density and the velocity are considered to be statistically independent as explained by VS [62]. This will be also confirmed by our DNS results shown in figure 5.4. The last term in (3.40) is the mixed product of a nonequilibrium and equilibrium displacement ($\langle z'\Delta z_{eq}\rangle$) and expected to be negligible for high Reynolds number flows (i.e. statistically independent) [42, 62]. The third term in (3.40) is also negligible for high Reynolds number. The remaining term is ε_p, thus, as the equilibrium level changes from $z_{eq}(0)$ to $z_{eq}(t)$, APE is converted to RPE through ε_p. Since $\varepsilon_p > 0$, the energy accumulates in the form of RPE through Φ_m.

3.5.5 Evolution of Total Potential Energy

From (3.35) and (3.38), the evolution equation of the total potential energy of all the fluid particles is given by,

$$\frac{DE_{tp}}{Dt} = \frac{DE_{ap}}{Dt} + \frac{DE_{rp}}{Dt}$$

$$= B - \varepsilon_p + \Phi_m \tag{3.41}$$

where B is the buoyancy flux which is the reversible conversion between KE and APE, ε_p is the irreversible dissipation of APE and Φ_m is the accumulation of RPE.

Combining (3.41) with (3.40) for high Reynolds flow gives,

$$\frac{DE_{tp}}{Dt} = B \tag{3.42}$$

The rate of change of TPE is controlled by the buoyancy flux, i.e, the rate of conversion from TKE. The form of TPE equation in (3.42) is same as that of an adiabatic case, thus the rate is independent of molecular diffusion. However, energy is continuously converted among TKE, APE and ultimately to RPE. The rate of conversion of APE to RPE is ε_p which will thus control the *relative* magnitudes of the PE components, APE and RPE.

3.6 Summary of Energetics

We may now describe the energy transfer and conversions using the TKE and PE evolution equations defined above. From (3.33), (3.35), and (3.38) the
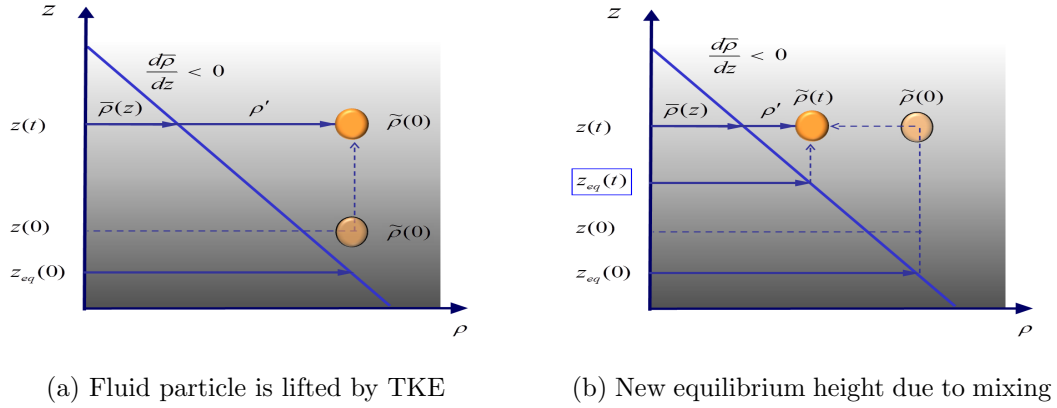
(a) Fluid particle is lifted by TKE

(b) New equilibrium height due to mixing

Figure 3.4: Sequence of processes

energetics of fluid particles are given by,

$$\frac{DE_k}{Dt} \;=\; -\rho_o\langle u'w'\rangle\frac{d\overline{U}}{dz} \;-\; \varepsilon_k \;-\; g\langle\rho'w'\rangle \tag{3.43}$$

$$\frac{DE_{ap}}{Dt} \;=\; \langle g\rho'w'\rangle \;-\; \frac{\kappa g}{d\overline{\rho}/dz}\langle\rho'\nabla^2\widetilde{\rho}\rangle \;=\; B \;-\; \varepsilon_p \tag{3.44}$$

$$\frac{DE_{rp}}{Dt} \;=\; \frac{\kappa g}{-d\overline{\rho}/dz}\langle\Delta\widetilde{\rho}\nabla^2\widetilde{\rho}\rangle \;=\; \Phi_m \tag{3.45}$$

$$\approx\; \frac{\kappa g}{d\overline{\rho}/dz}\langle\rho'\nabla^2\widetilde{\rho}\rangle$$

The above equations indicate that TKE is produced/maintained by mean shear $(-\rho_o\langle u'w'\rangle\frac{d\overline{U}}{dz})$ and some of this energy maybe be converted to APE reversibly through the buoyancy flux $g\langle\rho'w'\rangle$ or dissipated through ε_k.

The equations also indicate a sequence of processes associated with PE as illustrated in figure 3.4. In figure 3.4a, a fluid particle is released at $z(0)$ with $\widetilde{\rho}(0)$ and transported to $z(t)$ by w'. This initial buoyancy flux, $(\widetilde{\rho}(0) - \overline{\rho}(z))gw'$, converts energy in the form of TKE to APE. In figure 3.4b, the deviation from the surrounding/background density drives the molecular diffusion which then alters

the density of the fluid particle from $\widetilde{\rho}(0)$ to $\widetilde{\rho}(t)$, hence the equilibrium height changes from $z_{eq}(0)$ to $z_{eq}(t)$. This decreases ρ' and the associated APE and, correspondingly increases Δz_{eq} and associated RPE, i.e., APE is converted to RPE. The dissipated energy associated with ε_p is accumulated in the form of the unavailable potential energy, RPE, through Φ_m associated with the change in equilibrium reference height. This sequence of processes will be verified with DNS results in chapter 5.

Overall, from (3.43) and (3.44), the total turbulence energy, $E = E_k + E_{ap}$, is given by,

$$\frac{DE}{Dt} = -\rho_o \langle u'w' \rangle \frac{d\overline{U}}{dz} - \varepsilon_k - \varepsilon_p \tag{3.46}$$

Thus in stratified flows, there are two ways, ε_k and ε_p, by which the turbulence ultimately decays and the associated energy is transformed into the nonrecoverable forms of internal energy and RPE which may also be considered as internal energy as discussed in chapter 2. The fully Lagrangian energetics is now developed, and will be used to evaluate the vertical displacements of fluid particles.

The text of this dissertation includes the reprints of the following paper, submitted for consideration at the time of publication.

Chapter 3: Seungbum Jo, Keiko K. Nomura and James W. Rottman., 'The Lagrangian energetics of a fluid particle in a Boussinesq flow'., in preparation for submission for publication.

Chapter 4

Vertical Dispersion in Stratified Turbulent Flow

In this chapter, we derive equations for the mean square vertical displacement σ_{zp}^2 by applying our Lagrangian energetics analysis to a homogeneous stably stratified turbulent shear flow. In particular, the APE and RPE are related to the corresponding components of σ_{zp}^2 and their evolution equations are used to determine the behavior of $\sigma_{zp}^2(t)$. Thus, the Lagrangian energetics analysis is a more systematic approach for determining $\sigma_{zp}^2(t)$ and clarifies the role and significance of molecular mixing in the vertical dispersion of fluid particles in stratified flow. At the end, we will compare our dispersion model to some existing models for decaying and stationary turbulence.

4.1 Vertical Displacements: Relation to PE components

There are two ways to relate PE components to vertical displacements. First, we can use the Taylor series expansion [44]. Expansion of (3.7) for APE density in small $z'(z' = z - \Delta z_{eq})$ gives

$$\mathcal{E}_{ap} = -g\left(\frac{1}{2}\frac{\partial \rho_r}{\partial z}z'^2 + \frac{1}{3!}\frac{\partial^2 \rho_r}{\partial z^2}z'^3 + higher\ order\right) \tag{4.1}$$

For the uniform density profile in stably stratified turbulence, $\frac{d^2\rho_r}{dz^2}$ and all the higher order terms become zero since the background density$(\rho_r(z))$ is equal to mean density$(\overline{\rho}(z))$ for which the gradient is constant. Finally, the local APE density equation has a quadratic form and it is proportional to $\frac{1}{2}z'^2$,

$$\mathcal{E}_{ap} = -\frac{g}{2}\frac{\partial\overline{\rho}}{\partial z}z'^2 = \rho_o N^2 \frac{z'^2}{2} \tag{4.2}$$

Another way to express the APE density in terms of the square of vertical displacement is using the geometry of $\rho - z$ diagram. In figure 4.2, the triangle area represents the APE density in the uniformly stratified flow and this can be expressed in terms of the difference in the two areas indicated in figure 4.1. From (3.21),

$$\begin{aligned}
\mathcal{E}_{ap} &= \underbrace{g\int_{z_{eq}(t)}^{z(t)}\widetilde{\rho}(t)\,d\hat{z}}_{Area\ 1\ in\ 4.1a} - \underbrace{g\int_{z_{eq}(t)}^{z(t)}\overline{\rho}(\hat{z})\,d\hat{z}}_{Area\ 2\ in\ 4.1b} \\
&= \frac{1}{2}g\rho'z' = \frac{1}{2}g[z'(-\frac{d\overline{\rho}}{dz})]z' \\
&= \rho_o N^2\frac{z'^2}{2} \tag{4.3}
\end{aligned}$$

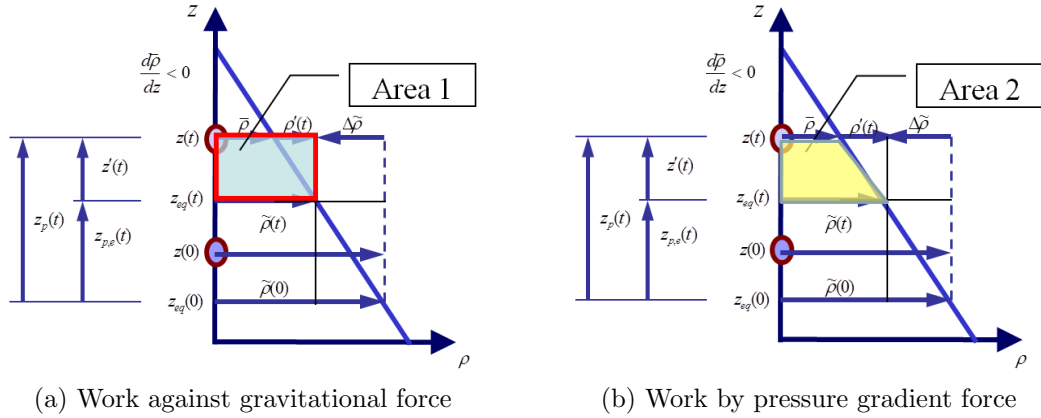(a) Work against gravitational force   (b) Work by pressure gradient force

Figure 4.1: Graphical representation of terms in APE density equation (4.3)
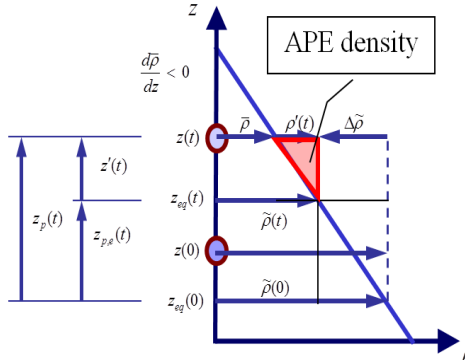

Figure 4.2: Graphical representation of APE density (= Area1 − Area2 in figure 4.1) in the Lagrangian framework

where $N^2 = -\frac{g}{\rho_o}\left(\frac{d\bar{\rho}}{dz}\right)$. Equation (4.3) yields the same result as (4.2) and the APE density is expressed in terms of nonequilibrium displacement squared.

Similarly, we may apply the graphical approach to relate RPE density to the equilibrium displacement. In figure 4.4, the triangle area represents RPE density and this can be expressed in terms of the difference in two areas indicated
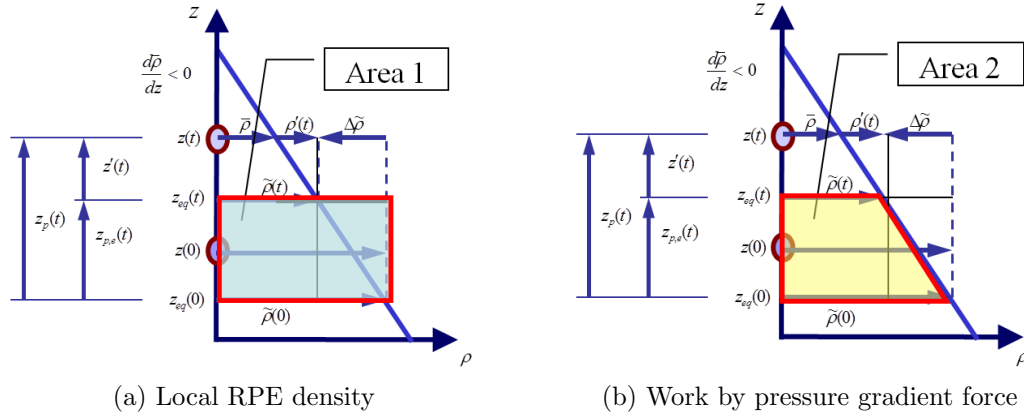
(a) Local RPE density   (b) Work by pressure gradient force

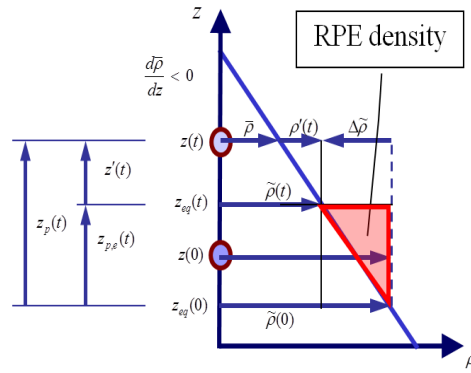Figure 4.3: Graphical representation of terms in RPE density equation (4.4)

Figure 4.4: Graphical representation of RPE density ($=$ Area1 $-$ Area2 in figure 4.3) in the Lagrangian framework

in figure 4.3. From (3.22),

$$
\begin{aligned}
\mathcal{E}_{rp} &= \underbrace{g \int_{z_{eq}(0)}^{z_{eq}(t)} \widetilde{\rho}(0)\, d\hat{z}}_{Area\ 1\ in\ 4.3a} - \underbrace{g \int_{z_{eq}(0)}^{z_{eq}(t)} \overline{\rho}(\hat{z})\, d\hat{z}}_{Area\ 2\ in\ 4.3b} \\
&= -\frac{1}{2} g \Delta \widetilde{\rho} \Delta z_{eq} = -\frac{1}{2} g [\Delta z_{eq}(-\frac{d\overline{\rho}}{dz})] \Delta z_{eq} \\
&= \rho_o N^2 \frac{\Delta z_{eq}^2}{2}
\end{aligned}
\tag{4.4}
$$

From (3.9), the TPE density in the uniform stratified flow can be expressed as the sum of APE and RPE density, and thus, using (4.3) and (4.4), the square

of nonequilibrium and equilibrium vertical displacements.

$$
\begin{aligned}
\mathcal{E}_{tp} &= \int_{z_{eq}(t)}^{z(t)} g(\widetilde{\rho}(t) - \overline{\rho}(\hat{z}))\, d\hat{z} + \int_{z_{eq}(0)}^{z_{eq}(t)} g(\widetilde{\rho}(0) - \overline{\rho}(\hat{z}))\, d\hat{z} \\
&= \rho_o N^2 \frac{z'^2}{2} + \rho_o N^2 \frac{\Delta z_{eq}^2}{2}
\end{aligned}
\tag{4.5}
$$

4.2 Mean Square Vertical Displacement

We now consider the behavior of the mean square vertical displacement, $\sigma_{zp}^2(t) \equiv \langle z_p^2(t) \rangle$, with high Re. Taking an ensemble average of (4.5) over all particles gives,

$$
\langle \mathcal{E}_{tp} \rangle = E_{tp} = \rho_o N^2 \frac{\sigma_{zp}^2}{2} = \rho_o N^2 \frac{\langle z'^2 \rangle}{2} + \rho_o N^2 \frac{\langle \Delta z_{eq}^2 \rangle}{2}
\tag{4.6}
$$

As indicated in chapter 3 for (3.45), we note that for high Reynolds number flows, it is expected that the mixed product ($\langle z' \Delta z_{eq} \rangle$) to be zero (i.e. statistically independent) [42, 62]. In (4.6), the mean square of vertical displacement of fluid particles is expressed in terms of the nonequilibrium displacement z' associated with the APE and equilibrium displacement Δz_{eq} associated with the RPE.

4.2.1 Energetics of Mean Square Vertical Displacement

Recall equations (3.43) - (3.45) describe the energetics of the fluid particles, in terms of the ensemble mean TKE, APE and RPE,

$$
\frac{DE_k}{Dt} \; = \; -\rho_o \langle u'w' \rangle \frac{d\overline{U}}{dz} \; - \; \varepsilon_k \; - \; g \langle \rho'w' \rangle \tag{3.43}
$$

$$
\frac{DE_{ap}}{Dt} \; = \; \frac{D}{Dt}\left(\rho_o N^2 \frac{\langle z'^2 \rangle}{2} \right) \; = \; \langle g\rho'w' \rangle \; - \; \frac{\kappa g}{d\overline{\rho}/dz}\langle \rho'\nabla^2 \widetilde{\rho} \rangle \; = \; B \; - \; \varepsilon_p \tag{3.44}
$$

$$
\frac{DE_{rp}}{Dt} \; = \; \frac{D}{Dt}\left(\rho_o N^2 \frac{\langle \Delta z_{eq}^2 \rangle}{2} \right) \; = \; \frac{\kappa g}{-d\overline{\rho}/dz}\langle \Delta\widetilde{\rho}\nabla^2 \widetilde{\rho} \rangle \; = \; \Phi_m \tag{3.45}
$$

$$
\approx \; \frac{\kappa g}{d\overline{\rho}/dz}\langle \rho'\nabla^2 \widetilde{\rho} \rangle
$$

From the energetics point of view, the amount of TPE does not change due to molecular diffusion as long as the same amount of energy is supplied from TKE since $\varepsilon_p \approx \Phi_m$. However, the energy is continuously converted between APE and RPE due to molecular diffusion and the relative magnitude of each PE components, APE and RPE, changes, hence the associated vertical displacement components change.

In the dispersion point of view, as the fluid particles move away from their original equilibrium level, TPE increases as TKE is converted reversibly to APE. If there is no molecular diffusion, the fluid particles tends to return to the original equilibrium level due to buoyancy force and are constrained to oscillate about the equilibrium level. As fluid particles change their density through molecular diffusion and thus alters equilibrium levels, APE is dissipated and eventually converted irreversibly into RPE where the energy accumulates. The fluid particles can

thereby move further away from their original equilibrium levels and now oscillate about the new equilibrium level.

4.2.2 Model for Mean Square Vertical Displacement

Time integration of (3.41) with (3.38) and (4.6) gives,

$$
\int_0^t \frac{DE_{tp}}{Dt}\, dt \;=\; \int_0^t \frac{DE_{ap}}{Dt}\, dt \;+\; \int_0^t \frac{DE_{rp}}{Dt}\, dt
$$

$$
\int_0^t \frac{D}{Dt}\left(\rho_o N^2 \frac{\langle z_p^2 \rangle}{2}\right) dt \;=\; \int_0^t \frac{D}{Dt}\left(\rho_o N^2 \frac{\langle z'^2 \rangle}{2}\right) dt \;+\; \int_0^t \frac{D}{Dt}\left(\rho_o N^2 \frac{\langle \Delta z_{eq}^2 \rangle}{2}\right) dt
$$

$$
\rho_o N^2 \frac{\langle z_p^2 \rangle}{2} \;=\; \rho_o N^2 \frac{\langle z'^2 \rangle}{2} + \int_0^t \Phi_m\, dt
$$

$$
\sigma_{zp}^2(t) \;=\; \langle z'^2 \rangle \;+\; \frac{2}{\rho_o N^2}\int_0^t \Phi_m\, dt \tag{4.7}
$$

where $E_{tp}(0) = E_{ap}(0)$, hence, $\langle z_p(0)^2 \rangle = \langle z'(0)^2 \rangle$ since initially there is no change in the reference state and all of TPE exists as APE.

Thus, if there is no diffusion ($\Phi_m = 0$), fluid particles are constrained to oscillate about their equilibrium level and $\sigma_{zp}^2(t) = \langle z'^2 \rangle$. However, with molecular diffusion, from (4.7), since the integral of Φ_m grows in time, σ_{zp}^2 will grow without limit. As noted earlier, it must be kept in mind that the complete dynamics are described by the coupled system given by (3.24) and (3.33). As $N^2 (= -\frac{g}{\rho_o}\left(\frac{d\bar{\rho}}{dz}\right))$ decreases, the influence of ρ' on the velocity field is diminished. In the limit of $N^2 \to 0$, $E_{tp} \to 0$; potential energy considerations are no longer relevant. In this limit, ρ' is a passive scalar and (4.7) simply describes the *one-way response* of the scalar field to the flow. The velocity field is decoupled from the scalar field; $\sigma_{zp}^2(t)$

is described solely by the velocity and the energetics of σ_{zp}^2 are confined to kinetic energy considerations.

4.2.3 Non-dimensionalized Mean Square Vertical Displacement

The above ideas motivate scaling in terms of energy quantities. Nondimensionalizing (4.7) with the initial total turbulence energy, $E(0) = E_k(0) + E_{ap}(0)$,

$$\sigma_{zp}^{*2}(t) \;=\; \frac{\rho_o N^2 \, \sigma_{zp}^2(t) \,/2}{E(0)} \;\;=\;\; \frac{\rho_o N^2 \, \langle z'^2(t)\rangle/2}{E(0)} \;+\; \frac{\int_0^t \Phi_m(t)\,dt}{E(0)} \;, \qquad (4.8)$$

i.e.,

$$E_{tp}^*(t) \;\;=\;\; E_{ap}^*(t) \;+\; E_{rp}^*(t) \;, \qquad (4.9)$$

where the asterisks denote the non-dimensional quantities. The mean square displacement is thereby considered in terms of non-dimensional potential energy components (4.9). We may also express (4.9) as,

$$
\begin{aligned}
E_{tp}^*(t) \;\;&=\;\; E_{ap}^*(t) \;+\; \frac{\int_0^t \Phi_m(t)\,dt}{E(0)} \\
&=\;\; E_{ap}^*(t) \;+\; \Omega_c(t) \int_0^t \frac{\varepsilon(t)}{E(0)}\,dt
\end{aligned}
\qquad (4.10)
$$

where $\varepsilon \;=\; \varepsilon_k + \varepsilon_p$ is the total rate of dissipation of turbulence energy and Ω_c is a *cumulative mixing efficiency* which is the ratio of mixing rate to the total dissipation rate [41]. This shows how much of turbulent energy is used for mixing.

$$\Omega_c(t) \;\;=\;\; \frac{\int_0^t \Phi_m(t)\,dt}{\int_0^t \varepsilon(t)\,dt} \qquad (4.11)$$

As discussed in VS, the mixing efficiency is a measure of the portion of turbulence energy that goes into changing the potential energy of the fluid by irreversible mixing thereby quantifying the significance of stratification in transient mixing events. In general, significant dispersion and scalar variance dissipation may occur in a flow. How influential the latter is on the former in stratified flow may be indicated by Ω_c.

4.3   Long Time Behavior

In (4.7), at large times, since $\langle \Delta z_{eq}^2 \rangle$ is a cumulative quantity , we expect $\langle \Delta z_{eq}^2 \rangle \gg \langle z'^2 \rangle$. This is consistent with the observed behavior in VS [62] that the equilibrium displacement dominates the vertical displacement even in weakly stratified flow. We now consider two limiting flow conditions for long time in more detail.

4.3.1   Decaying turbulence

In the case of decaying turbulence, all of the turbulence energy eventually dissipates; as $t \to \infty$, $E_k(t)$, $E_{ap}(t) \to 0$. TPE then exists all in the form of RPE and (4.10) may be written as,

$$E_{tp}^*(\infty) \;=\; E_{rp}^*(\infty) \;=\; \Omega_c(\infty) \frac{E(0) + E_{sh}(\infty)}{E(0)} \tag{4.12}$$

where $E_{sh}(\infty)$ is the total TKE produced by shear,

$$E_{sh}(\infty) \; = \; - \int_0^\infty \rho_o \langle u'w' \rangle \frac{d\overline{U}}{dz} \, dt \qquad (4.13)$$

For unsheared decaying flow $(E_{sh} = 0)$,

$$E_{tp}^*(\infty) \; = \; \Omega_c(\infty) \; . \qquad (4.14)$$

Thus, in decaying flows (with and without shear) at long time, σ_{zp}^{*2} approaches a constant corresponding to the total change in potential energy that occurred in the fluid by irreversible mixing. The final state is at equilibrium with minimum potential energy, E_{rp}^*.

4.3.2   Stationary turbulence

In the case of stationary turbulence, E_k, E_{ap}, $\langle \rho'w' \rangle$, ε_p, Φ_m, and ε are maintained constant in the flow. For these conditions, the growth rate of TPE is equal to that of the RPE which is given by the equilibrium mixing rate, Φ_m. Integrating (4.10) and (4.11) with constant equilibrium mixing rates yields,

$$E_{tp}^*(t^*) \; = \; E_{ap}^* \; + \; \Omega_c \, t^* \qquad (4.15)$$

where $\Omega_c = \Omega = \Phi_m/\varepsilon$ is a (constant) instantaneous mixing efficiency, $t^* = t/T_L$, and $T_L = E/\varepsilon$ is the turbulence energy decay time. In stationary flow, TKE is continually converted to APE. Since the time at which particles are identified is arbitrary, at any selected initial time $(t = 0)$, all of the TPE exists as APE, $E_{tp}^*(0) = E_{ap}^*$. As time proceeds and diffusion occurs, APE is dissipated at a rate

given by ε_p and eventually converted to RPE at a rate of Φ_m, hence, TPE increases in time through these energy conversion processes.

4.4 Time scale for stationary turbulence

Since APE maintains constant, the analysis yields a simple model for $\sigma_{zp}^2(t)$ for stationary turbulence for which we have,

$$\frac{D\sigma_{zp}^2}{Dt} = \frac{D\langle \Delta z_{eq}^2 \rangle}{Dt} = \frac{2\,\varepsilon_\rho}{(d\bar{\rho}/dz)^2} = 2\,K_d \tag{4.16}$$

and K_d is the diapycnal turbulent diffusivity. The resulting $\sigma_{zp}^2(t)$ may be scaled as,

$$\frac{\sigma_{zp}^2(t)}{L_E^2} = 1 + \frac{t}{T_\rho}\,, \tag{4.17}$$

where $L_E^2 = \rho'^2/(d\bar{\rho}/dz)^2$ is the Ellison overturn scale, and $T_\rho = \rho'^2/2\varepsilon_\rho$ is the decay timescale for density fluctuations. We may also write (4.17) as,

$$z_p^{*2} \equiv \frac{\sigma_{zp}^2(t)}{L_E^2} = 1 + 2\gamma'\frac{t}{T_k}\,, \tag{4.18}$$

where $T_k = E_k/\varepsilon_k$ is the decay timescale for TKE and

$$2\gamma' = \frac{T_k}{T_\rho}\,, \tag{4.19}$$

is the ratio of the mechanical to scalar timescales, a parameter used in second order closure models. As discussed in VS, γ' is relatively insensitive to stratification and may vary slowly with Re and Pr. Thus, if γ' is independent of stratification, an effective timescale for vertical dispersion is T_k.

4.5 Dispersion Model Comparison

4.5.1 Comparison to LB model

Lindborg & Brethouwer [5] derived the equation for mean square vertical displacement by integrating evolution equation for buoyancy flux with an assumption of negligible of $\kappa \langle w' \nabla^2 \rho'(t) \rangle$.

$$
\begin{aligned}
\langle \sigma_{zp}^2(t) \rangle &= \frac{2}{\rho_o N^2} \int_0^t \left(\langle g \rho'(t') w' \rangle - \langle g \rho'(0) w' \rangle \right) dt' \qquad (4.20) \\
&= \frac{2}{\rho_o N^2} \int_0^t \left(\langle g \rho'(t') w' \rangle - \varepsilon_p(t') + \varepsilon_p(t') - \langle g \rho'(0) w' \rangle \right) dt' \\
&= \frac{2}{\rho_o N^2} \left(E_{ap}(0) + E_{ap}(t') - \langle g \rho'(0) z'(t') \rangle + \int_0^t \varepsilon_p(t') \, dt' \right) \quad (4.21)
\end{aligned}
$$

where E_{ap} is an available potential energy and ε_p is the dissipation rate of APE

LB's model for mean square vertical displacement with the zero initial density fluctuation $\rho'(0) = 0$ in (4.21) is consistent with the derived equation (4.7) since the dissipation rate of APE is equal to mixing rate of RPE, i.e., $\varepsilon_p \approx \Phi_m$.

Although LB's model for mean square vertical displacement is same as our model, the physical interpretations were not entirely clear since they did not explicitly consider the energetics.

Long time behavior comparison - Decaying turbulence

LB [5] derived the long time expression for decaying and stationary turbulence from (4.21). For decaying case, as $t \to \infty$, the last term in (4.21) goes to a constant value which is the total dissipated amount of potential energy and LB

consider it as a some fraction of the total initial energy, $E_k(0) + E_{ap}(0)$. The two middle terms in (4.21) go to zero as $t \to \infty$ since there is no available potential energy after all for decaying turbulence. Thus,

$$\langle \sigma_{zp}^2(\infty) \rangle \quad = \quad \frac{2}{\rho_o N^2}[E_{ap}(0) + a(E_k(0) + E_{ap}(0))] \qquad (4.22)$$

where a is a value between 0 and 1 and varies with an initial condition but the variable "a" is not clearly interpreted.

Non-dimensionalized by initial total energy of (4.22) gives,

$$\langle \sigma_{zp}^2(\infty) \rangle^* \quad = \quad a + E_{ap}(0)^* \qquad (4.23)$$

LB's model for decaying turbulence in (4.23) is consistent with our derived model in (4.14) and the variable "a" in (4.23) is identified as mixing efficiency $(\Omega_c(\infty))$. The non-dimensionalized initial APE $(E_{ap}(0)^*)$ will be eventually converted to RPE, hence this term should be also accounted into variable "a".

Long time behavior comparison - Stationary turbulence

For the case of stationary turbulence, LB derived the expression for long time behavior from (4.21) by assuming that the adiabatic dispersion reaches its upper bound $\langle \delta z'^2 \rangle = 4E_{ap}/(\rho_o N^2)$ [29].

$$\langle \sigma_{zp}^2(\infty) \rangle \quad = \quad \frac{1}{\rho_o N^2}[4E_{ap} + 2\varepsilon_p t] \qquad (4.24)$$

Equation (4.24) is rewritten by scaling of $4E_P/\rho_o N^2$ and gives,

$$\langle \sigma_{zp}^2(\infty) \rangle^* \quad = \quad 1 + \frac{1}{2}t^{**} \qquad (4.25)$$

where $t^{**} = t/T$ and $T = E_{ap}/\varepsilon_p$ is eddy turnover time

In the case of no initial fluctuation, i.e., $z'(0) = 0$, hence, $\langle \delta z'^2 \rangle = \langle z'(t)^2 \rangle -$

$2\langle z'(t)z'(0) \rangle + \langle z'(0)^2 \rangle = \langle z'(t)^2 \rangle = 2E_{ap}/(\rho_o N^2)$. However, in (4.24), $\langle \delta z'^2 \rangle$ is

assumed to be equal to $4E_{ap}$ which indicates that E_{ap} is proportional to $\frac{1}{4}z'^2$. This

assumption is against the general idea that APE is proportional to $\frac{1}{2}z'^2$ [14].

If (4.24) is scaling by $2E_{ap}/\rho_o N^2$ with a correction of $\langle \delta z'^2 \rangle = 2E_{ap}/(\rho_o N^2)$,

the mean square vertical displacement gives,

$$\langle \sigma_{zp}^2(\infty) \rangle^* = 1 + t^{**} \tag{4.26}$$

Same scaling application to our model

Our model for stationary case in (4.7) can be written by scaling of $2E_{ap}/\rho_o N^2$

as LB model in (4.26) combining with (4.3), $E_{ap} = \rho_o N^2 \frac{\langle z'^2 \rangle}{2}$.

$$
\begin{aligned}
\sigma_{zp}^2(t) &= \langle z'^2 \rangle + \frac{2}{\rho_o N^2} \int_0^t \Phi_m \, dt \\
\frac{\sigma_{zp}^2(t)}{2E_{ap}/\rho_o N^2} &= 1 + \frac{\Phi_m}{E_{ap}} t \\
\sigma_{zp}^2(t)^* &= 1 + t^*
\end{aligned}
\tag{4.27}
$$

where $t^* = t/T_m$, and $T_m = E_{ap}/\Phi_m$ is the turbulence mixing time.

Now the corrected LB model for stationary turbulence at long time in (4.26)

is consistent with our model in (4.27).

4.5.2 Reconsideration of PPH model

With our results for stationary flow, we now reconsider the model of PPH (1.7), which assumes that small-scale mixing scales with the buoyancy time scale, i.e.,

$$\gamma \;=\; \frac{1/N}{\overline{\rho'^2}/\varepsilon_\rho} \tag{4.28}$$

As shown by VS, γ varies with N and thus (4.28) is not the appropriate scaling; rather, the timescale for small-scale mixing should be related to that of the energy decay, i.e., γ' (4.19). Using γ' (4.19) as a modified mixing parameter in place of γ (4.28) in the derivation of the Langevin formulation of PPH gives the following result,

$$\sigma_z^{*2} \;=\; \frac{\langle (\Delta z)^2 \rangle}{\langle w'^2 \rangle / N^2} \;=\; \zeta_z^2 \;+\; \frac{2\gamma'^2}{N^2 T_k{}^2}\, Nt \;=\; \zeta_z^2 \;+\; 2\gamma'^2\, Fr^2\, Nt \;. \tag{4.29}$$

which, as expected, differs from the original result (1.7) by the growth rate factor.

We can compare the modified PPH relation (4.29) with our energetics analysis result (4.18). Non-dimensionalizing (4.18) with VKE and buoyancy time scales gives,

$$\sigma_{zp}^{*2} \;=\; \frac{\langle z_p^2 \rangle}{\langle w'^2 \rangle / N^2} \;=\; \beta \left[1 \;+\; \frac{2\gamma'}{NT_k}\, Nt \right] \;=\; \beta(1 \;+\; 2\gamma' Fr\, Nt) \;, \tag{4.30}$$

where $Fr = (1/N)/T_k$ and $\beta = L_E^2/(\langle w^2 \rangle / N^2)$ is a nondimensional amplitude. We see that the growth rate factor $\gamma' Fr$ differs from that in (4.29) by a power of 2. A similar observation was noted by Kimura and Herring[24] with their Langevin model results.

The various model growth rates may be compared quantitatively. For the original PPH model (1.7) and using the bounds for typical γ values ($\gamma = 0.1, 0.4$), $0.02 \leq 2\gamma^2 \leq 0.32$. For the modified PPH model (4.29) with the DNS parameter values, $2\gamma'^2 Fr^2 = 0.229 \pm 0.063$. For our developed model (4.30) with the DNS parameter values, $2\beta\gamma' Fr = 0.616 \pm 0.087$, which agrees well with the simulation results which will be shown in chapter 5. The predicted growth rates using the PPH model do not agree with the DNS results. The modified PPH model, with the timescale corrected, lies between the original PPH predictions, but still underpredicts the growth rates of the DNS flows.

4.6 Summary and conclusions

The two PE components are related to two vertical displacements respectively, i.e, the APE associated with a nonequilibrium displacement z' and the RPE associated with an equilibrium displacement Δz_{eq}. The total potential energy associated with the total displacement, z_p, is expressed in terms of z' and Δz_{eq}. In the uniform stratified flow ($\rho_r(z) = \overline{\rho}(z)$), the mean square vertical displacements is expressed as the sum of them, $\sigma_{zp}^2(t) = \langle z'^2(t) \rangle + \langle \Delta z_{eq}^2(t) \rangle$. As the fluid particles move away from their original equilibrium level, TPE increases as TKE is converted reversibly to APE. With molecular diffusion, fluid particles change their density and thus alters equilibrium levels. Hence, APE is dissipated and eventually converted irreversibly into RPE where the energy accumulates. The fluid

particles can thereby move further away from their original equilibrium levels and now oscillate about the new equilibrium level.

TPE (z_p^2) is dominated by RPE (Δz_{eq}^2) at long time for all cases, decaying, stationary and growing turbulence. However, since the increase in RPE is a direct result of energy conversion through APE, it does not dominate in the dynamical sense. In decaying turbulence, APE will eventually decay and what remains is the RPE accumulated during the transient event. The mean square vertical displacement σ_{zp}^2 equals the mean square equilibrium displacement $\langle \Delta z_{eq}^2 \rangle$ and approaches to a constant value given by the cumulative mixing efficiency $\Omega_c(\infty)$. In stationary turbulence, APE is maintained constant while RPE continually accumulates and grows. The mean square vertical displacement grows linearly in time at a rate given by the (constant) instantaneous mixing efficiency.

Lindborg and Brethouwer [29] derived similar relations for $\sigma_z^2(t)$ in which they consider the two terms on the right-hand side of (4.24) as the adiabatic and diabatic contributions, respectively. In particular, the long-time growth rate from the diabatic contribution for stationary flow is the same as in (4.16) and, as they note, K_d corresponds to the diffusivity used in the model of Osborn and Cox [37]. However, Lindborg and Brethouwer [29] interpret the contributions by considering only APE associated with a nonequilibrium displacement, whereas our analysis considers both nonequilibrium and equilibrium displacement by developing full Lagrangian energetics. Also, this analysis more clearly recognizes that the processes are sequential in nature. That is, small-scale mixing acts to preserve displace-

ments and reduce the reconversion of potential energy to kinetic energy but is not, by itself, the predominant contributor of transport. Furthermore, we demonstrate the irreversibility of the nonequilibrium component, $\langle \Delta z_{eq}{}^2 \rangle$. Our model for stationary flow (4.17), given in terms of σ_{zp}^2, does not exhibit a dispersion plateau and is consistent with a constant scalar variance, E_{ap} as will be shown in chapter 5.

The text of this dissertation includes the reprints of the following paper, submitted for consideration at the time of publication.

Chapter 4: Keiko K. Nomura, James W. Rottman and Seungbum Jo., 'The energetics of vertical fluid particle dispersion in stably stratified turbulence'., in preparation for submission for publication.

Chapter 5

Numerical Results of Energetics

and Turbulent Dispersion

In this chapter, we examine the ideas and relations from our energetics and turbulent dispersion analysis using DNS (Direct Numerical Simulation) of homogeneous stably stratified shear flow. The behavior of the flow and associated energetics have previously been studied in terms of Eulerian statistics [10, 12, 15, 21] and is well documented. The Lagrangian statistics are obtained by tracking a fluid particle. Here, we consider three flow cases, decaying, stationary and growing turbulence which Richardson number are 1.0, 0.13 and 0.01.

5.1 Results for stably stratified shear flow

5.1.1 Direct numerical simulations

The simulations performed follow those of Diamessis and Nomura [10]. Relevant nondimensional parameters include the turbulent Reynolds number based on the Taylor microscale, $Re_\lambda = v\lambda/\nu$, the Shear number, $Sh = SE_k/\varepsilon_k$, and the Prandtl number, $Pr = \nu/\kappa$. Here, v is the r.m.s turbulent velocity and $S \equiv dU/dz$ is the mean vertical velocity gradient. The relative significance of stratification to mean shear effects is characterized by the gradient Richardson number, $Ri = N^2/S^2$.

For given initial turbulent Reynolds number (Re_{λ_o}) and Shear number (Sh_o), the value of Ri (with respect to the critical Richardson number value, Ri_{cr}) designates distinct flow regimes: subcritical flow $(Ri < Ri_{cr})$ in which turbulence grows, critical flow $(Ri = Ri_{cr})$ in which turbulence is stationary, and supercritical flow $(Ri > Ri_{cr})$ in which turbulence decays.

Two sets of simulations, differing in initial conditions, were performed for this study. In the first set, the simulations were initialized with a fully developed isotropic turbulent velocity field and zero scalar fluctuations $(\rho'(0), E_{ap}(0) = 0)$. Thus, particle statistics exhibit an early time transient during which ρ'^2 is established. Initial parameter values for these runs are $Re_{\lambda_o} = 26$ and $Sh_o = 2.3$. In the second set, the simulations were initialized with nonzero initial scalar fluctuations $(\rho'(0), E_{ap}(0) \neq 0)$. For the fully stationary flow, buoyancy and shear are added to

fully developed isotropic turbulent velocity field. Statistics are then obtained after stationary flow conditions are achieved. For this flow, $Re_{\lambda,o} = 27$ and $Sh_o = 3.8$. In all simulations, $Pr = 0.7$.

Lagrangian statistics are obtained by a fluid particle tracking scheme based on cubic spline interpolation for the particle velocity from the available Eulerian flow field [71, 62]. Time integration for particle displacement (3.26) is carried out in the same manner as the Eulerian field. The total number of particles used is 4096. The particles are initially distributed uniformly in the computational domain. The presence of mean shear is handled as in Shen & Yeung [47] by subtracting the corresponding mean displacement of particles released from each horizontal plane. By doing so, only the displacement due to turbulence fluctuations is retained. In this method, single-particle displacement statistics may be equivalently viewed in an inertial frame that moves at the value of the mean velocity at the initial particle position [47].

5.1.2   Energetics statistics

Nondimensionalizing potential energy components with the initial total turbulent energy, $E(0)$, is given by,

$$
\begin{aligned}
\frac{E_{tp}}{E(0)} &= \frac{E_{ap}}{E(0)} + \frac{E_{rp}}{E(0)} \\
E_{tp}^*(t) &= E_{qp}^*(t) + E_{rp}^*(t)
\end{aligned}
\tag{5.1}
$$

where the asterisks denote the non-dimensional quantities.

The figure 5.1 shows the nondimensionalized potential energy components for three flow conditions, decaying, stationary and growing turbulent flow. The portion of PE components out of the total energy increases as the stratification becomes stronger whereas the total displacement is restricted with a strong stratification as shown in figure 5.3. This is consistent with VS's [62] idea which showed that the contribution from the potential energy dissipation (ε_p) becomes a significant portion of the total energy dissipation as the stratification becomes stronger. For all flow conditions, figure 5.1 shows TPE is dominated by APE at short time and RPE dominates TPE at long time as described in a mean square vertical displacement statistics. The figure 5.2 shows the non-dimensionalized mixed products (defined as MP) of z' and Δz_{eq} (denoted by $E_{mp}^* = \rho_o N^2 \frac{<z'\Delta z_{eq}>}{E(0)}$) and E_{mp}^*, is small compared to E_{tp}^* for all flow conditions.

Figures 5.3 and 5.4 show the time development of the $E_{tp}^*(t)$ components and the terms of the corresponding evolution equations (3.35) and (3.38), respectively, for the first set of simulations ($E_{ap}(0) = 0$). In the supercritical flow ($Ri = 1.0$, figure 5.3a), TKE decays in time; E_{tp}^* initially grows as E_{ap}^* develops and then decreases as E_{ap}^* decays. Correspondingly, $g\langle\rho' w'\rangle$ initially increases and then decreases even becoming negative before eventually diminishing in value (figure 5.4a). As E_{ap}^* is established, E_{rp}^* develops; the rate of growth decreasing as E_{ap}^* decreases. At long time, $E_{ap}^* \to 0$ and $E_{tp}^* \to E_{rp}^*$ (4.12) which approaches a constant value of approximately 0.17. In the critical flow ($Ri = 0.13$, figure 5.3b),

beyond the initial transient, TKE is maintained nearly constant and E_{tp}^* exhibits a nearly linear growth. During this time, $g\langle \rho' w'\rangle$ and ε_p achieve an approximate balance (figure 5.4b) and E_{ap}^* remains nearly constant. The continual conversion of APE to RPE occurs at a constant rate (ε_p) and E_{rp}^* grows linearly in time as does the E_{tp}^*. In the subcritical flow ($Ri = 0.01$, figure 5.3c), TKE and TPE continually increase in time. In this case, $g\langle \rho' w'\rangle$ exceeds ε_p (figure 5.4c) which results in the growth of E_{ap}^*. We also observe that ε_p is comparable to the $\Delta \widetilde{\rho} \nabla^2 \rho'$ term (figure 5.4f); as E_{ap}^* is destroyed, E_{rp}^* increases at the same rate. As RPE accumulates, it eventually exceeds the APE (figure 5.3a, $St > 7$).

Figure 5.5 shows $E_{tp}^*(t)$ components and equation terms for the fully stationary flow ($Ri = 0.13$, $E_{ap}(0) \neq 0$). In this case, initially all of the TPE exists as APE. Since the flow is stationary, $g\langle \rho' w'\rangle$ and ε_p are in balance (figure 5.5b), and the APE remains constant for all time. We also observe that ε_p becomes comparable to the $\Delta \widetilde{\rho} \nabla^2 \rho'$ term. After a short time $St > 2 \sim T_\rho$, RPE increases nearly linearly, as does TPE (figure 5.5a). In contrast to the results of van Aartrijk et al.[60] and Brethouwer & Lindborg [5], a dispersion *plateau* does not develop (note that in our flow, $Re_b \approx 29$ and $Fr \approx 0.62$, which are comparable in value to those in Brethouwer & Lindborg). As discussed by Brethouwer & Lindborg [5], the development of the plateau in $\sigma_z^2(t)$ is associated with adiabatic dispersion, i.e., the nonequilibrium displacement, $z'(t) - z'(0)$, as indicated in (3.27). Thus, early in time, this quantity must develop (and decorrelate) from its initial value. The development of the plateau is thus dependent on initial conditions. This ar-

tifact is eliminated in the present analysis by defining the particle displacement with respect to $z_{eq}(0)$ (3.28). Our statistics for vertical dispersion $\sigma_{zp}^2(t)$, which do not exhibit this early time development, are consistent with stationary turbulence (constant $\langle z'^2(t) \rangle$) conditions.

In general, we observe that the TPE is dominated by APE at short time and by RPE at long time. Physically, as the particles are advected away from their initial (equilibrium) position to regions of differing density, there is a reversible gain in potential energy in the form of APE. However, due to the action of molecular diffusion, density perturbations are eventually reduced as particles exchange density with neighboring fluid. This changes their equilibrium level which represents an irreversible retention of potential energy, i.e., RPE. In terns of the Eulerian flow field, in general there may be a corresponding change in background potential energy. In these simulations the turbulence is spatially homogeneous and the mean fields are decoupled from the flow. Mixing occurs throughout the domain, however there is no net change in the *spatially averaged* density and correspondingly, no change in the background potential energy. However, in the Lagrangian frame, individual fluid particles are identified and *distinguished* and each experiences some net diffusive flux. The physical increase in potential energy is then indicated by their measured (equilibrium) displacements.

In order to gain further insight, conditional statistics are obtained from the fully stationary flow. We extract the history for a subset of particles by employing conditional sampling of specific high amplitude events occuring at time $St = St_c$

($St_c = 7.5$ in these results). Figure 5.6a-c show the expected TPE component values and corresponding equation terms for those fluid particles exhibiting high amplitude (above rms value) positive buoyancy flux $\rho'w$ at $St = St_c$. We observe that the peak in $\rho'w$ at $St_c = 7.5$ (figure 5.6b) is followed by a peak in APE, and *subsequently*, a peak in $\rho'\nabla^2\rho'$ develops which results in an increase in $\Delta\widetilde{\rho}\nabla^2\rho'$. The latter results in the enhanced increase in RPE (figure 5.6a). Beyond these events, the particles return to the ensemble average values. Figure 5.6d-f show the expected TPE component values and corresponding equation terms for those fluid particles exhibiting high amplitude $\rho'\nabla^2\rho'$ at $t = t_c$. In this case, the peak in $\rho'\nabla^2\rho'$ at $St_c = 7.5$ (figure 5.6e), is *preceded* by peaks in APE and $\rho'w$, and also results in enhanced $\Delta\widetilde{\rho}\nabla^2\rho'$ (figure 5.6f). This again leads to an enhanced increase in RPE (figure 5.6c). These results illustrate the *sequence of processes* associated with energy conversion and vertical dispersion.

As discussed earlier, the significance of small-scale mixing on the overall energetics is indicated by the mixing efficiency, Ω_c. Figure 5.7 shows $\Omega_c(t)$ evaluated from the DNS flows (with $E_{ap}(0) = 0$). Although values of $\langle z_p^2 \rangle$ and $\langle \Delta z_{eq}^2 \rangle$ are highest in the weakly stratified (subcritical, $Ri = 0.01$) flows, the low values of Ω_c indicate that small-scale mixing has a relatively small effect on the total energy of the flow. As the stratification level increases (critical and supercritical flows), small-scale mixing has a stronger influence on σ_{zp}^2 as the increase in values of Ω_c indicate. In the decaying flow (figure 5.7a), $\Omega_c \approx 0.17$, which is comparable to expected values of mixing efficiency for decaying flows. We note that in the fully

stationary flow $(E_{ap}(0) \neq 0)$, $\Omega_c(t) \approx 0.14$.

Figure 5.8a shows z_p^{*2} versus t/T_k for the DNS results and the model (4.18) for which we use $\gamma' = 0.7$. The agreeement is quite good except for some deviation at late times due to development away from exact stationary conditions in our simulations. In particular, the measured long time slope from the DNS data is 1.42 ± 0.08. The corresponding γ' values, $0.67 - 0.75$, are comparable to those determined by VS for a range of stratification levels $(0 \leq Ri \leq 1000)$ in both unsheared [62] and shear flows.

Figures 5.8b,c show the comparison on log scale plots. The good agreement between the DNS results and model is also observed at early time. Figure 5.8c also shows the relative development of RPE within the timescale, T_k.

5.2   Summary and conclusions

In summary, the DNS results demonstrate our energetics analysis of dispersion, and in particular, the sequence of processes involved in (3.35) and (3.38) and the distinct roles of advection and diffusion in vertical particle displacement. From the Lagrangian analysis and DNS simulation results, we can verify that the RPE associated with a diapycnal displacement is dominant in TPE for all flow conditions. We conclude that in stably stratified stationary flow, the turbulent diffusivity K_ρ is directly related to the dispersion coefficient, K_z, which is equal to the rate of growth of mean square equilibrium displacement, $2K_d = D\langle \Delta z_{eq}^2 \rangle / Dt$.

The latter directly describes the effects of molecular diffusion on vertical transport and the underlying physical idea of PPH. The relevant time scale is that of the decay of density fluctuations, T_ρ, which is related to the kinetic energy decay time, T_k. This is consistent with the prevailing idea, as acknowledged by PPH and VS, that in high Re turbulent flows, the rate of small-scale mixing is not dependent on the molecular diffusivity. In general, the total vertical flux includes a contribution from molecular diffusion,

$$F_z \;=\; w\widetilde{\rho} - \kappa\nabla\widetilde{\rho} \tag{5.2}$$

and, as given in VS, the total diffusivity may be expressed by a general scaling relation,

$$\frac{K_d + \kappa}{\kappa} \;=\; 1 + \gamma'\frac{{L_E}^2}{T_k\,\kappa} \tag{5.3}$$

which indicates that the diffusivity reduces to the molecular value for low turbulent Peclet numbers, $Pe_t = {L_E}^2/T_k\,\kappa$.

In order to address the role of molecular diffusion on the buoyancy flux itself, the appropriate evolution equation to be considered is,

$$
\begin{aligned}
\frac{D\rho' w}{Dt} \;&=\; \rho'\frac{Dw}{Dt} + w\frac{D\rho'}{Dt} \\
&=\; \left[-\frac{\rho'}{\rho_o}\frac{\partial p}{\partial z} + \nu\rho'\nabla^2 w - \frac{g}{\rho_o}\rho'^2\right] + \left[w^2\left(-\frac{d\overline{\rho}}{dz}\right) + \kappa w\nabla^2\rho'\right]
\end{aligned} \tag{5.4}
$$

in which the last term corresponds directly to these effects. As noted in VS, we expect small-scale mixing to be independent of the velocity at high Reynolds numbers. Our DNS results indicate $\langle\kappa w\nabla^2\rho'\rangle$ to be small as shown in figure 5.9.

From our energetics analysis, we have formulated a dispersion model for stationary homogeneous turbulence. The model captures the basic long-time behavior of the PPH model of linear growth of $\langle z_p{}^2 \rangle$, however it differs in the underlying time scaling. Results for long time behavior and growth rate compare well with our DNS results for stationary homogeneous sheared turbulence. The PPH model, even with a correction in the mixing timescale, underpredicts the DNS flow results. This is attributed to the differing time scale exponent of 2, which is an outcome of their Langevin model formulation.
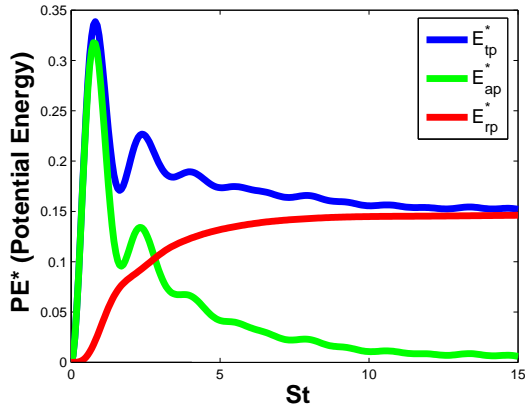
(a) Ri=5.0
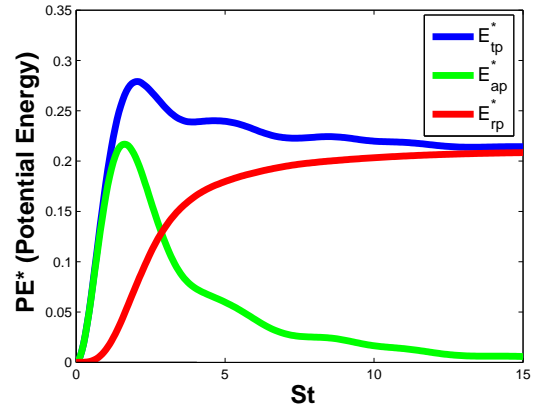
(b) Ri=1.0
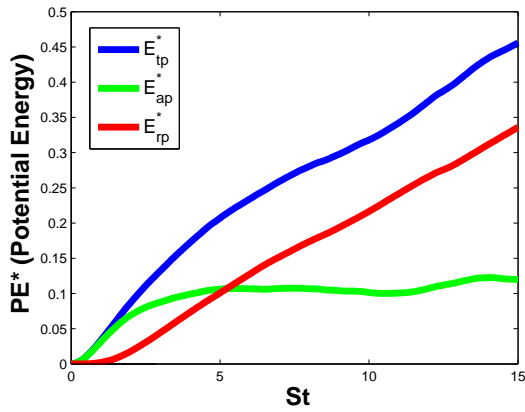
(c) Ri=0.135
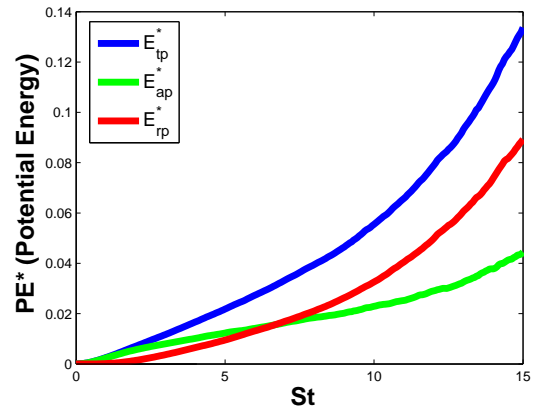
(d) Ri=0.01

Figure 5.1: Potential Energy Components for (a) Ri=5.0, (b) Ri=1.0, (c) Ri=0.13, (d) Ri=0.01. Green line : E_{tp}^*, Blue line : E_{ap}^*, Red line : E_{rp}^*
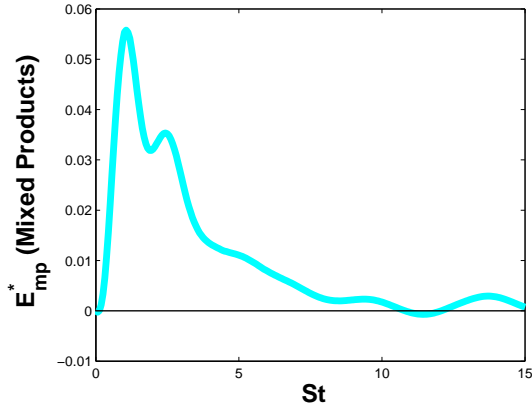
(a) Ri=5.0
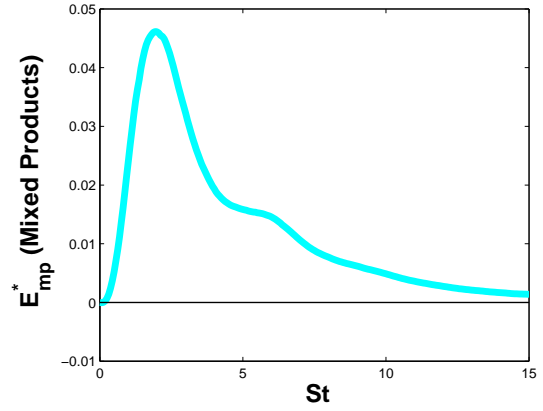
(b) Ri=1.0
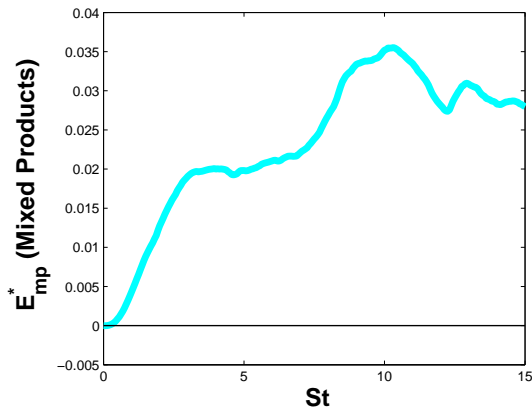
(c) Ri=0.135
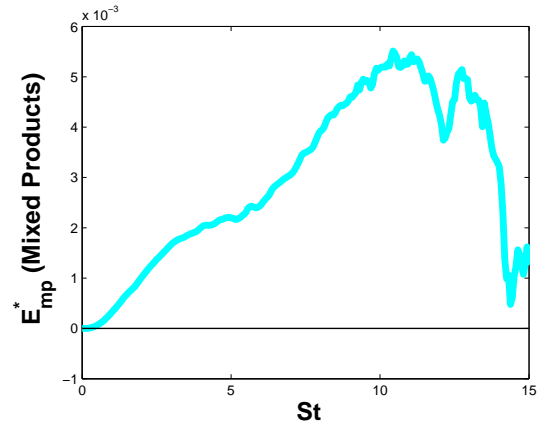
(d) Ri=0.01

Figure 5.2: Non-dimensionalized mixed products of z' and Δz_{eq} ($E^*_{mp} = \rho_o N^2 \frac{<z'\Delta z_{eq}>}{E(0)}$) for (a) Ri=5.0, (b) Ri=1.0, (c) Ri=0.13, (d) Ri=0.01.
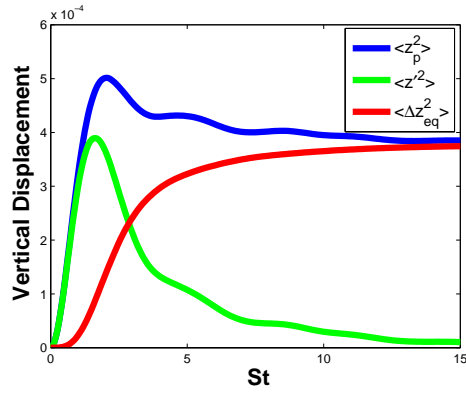
(a) Ri=1.0
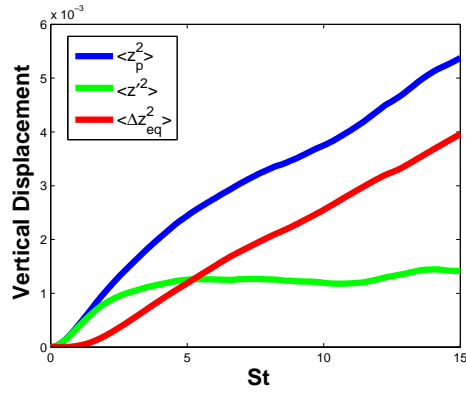
(b) Ri=0.13
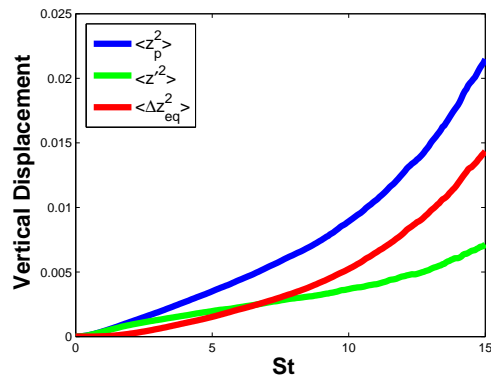
(c) Ri=0.01

Figure 5.3: Time development of mean square vertical displacement and components for (a) Ri=1.0, (b) Ri=0.13, (c) Ri=0.01. Green line : $< z_p^2 >$, Blue line : $< z'^2 >$, Red line : $< \Delta z_{eq}^2 >$
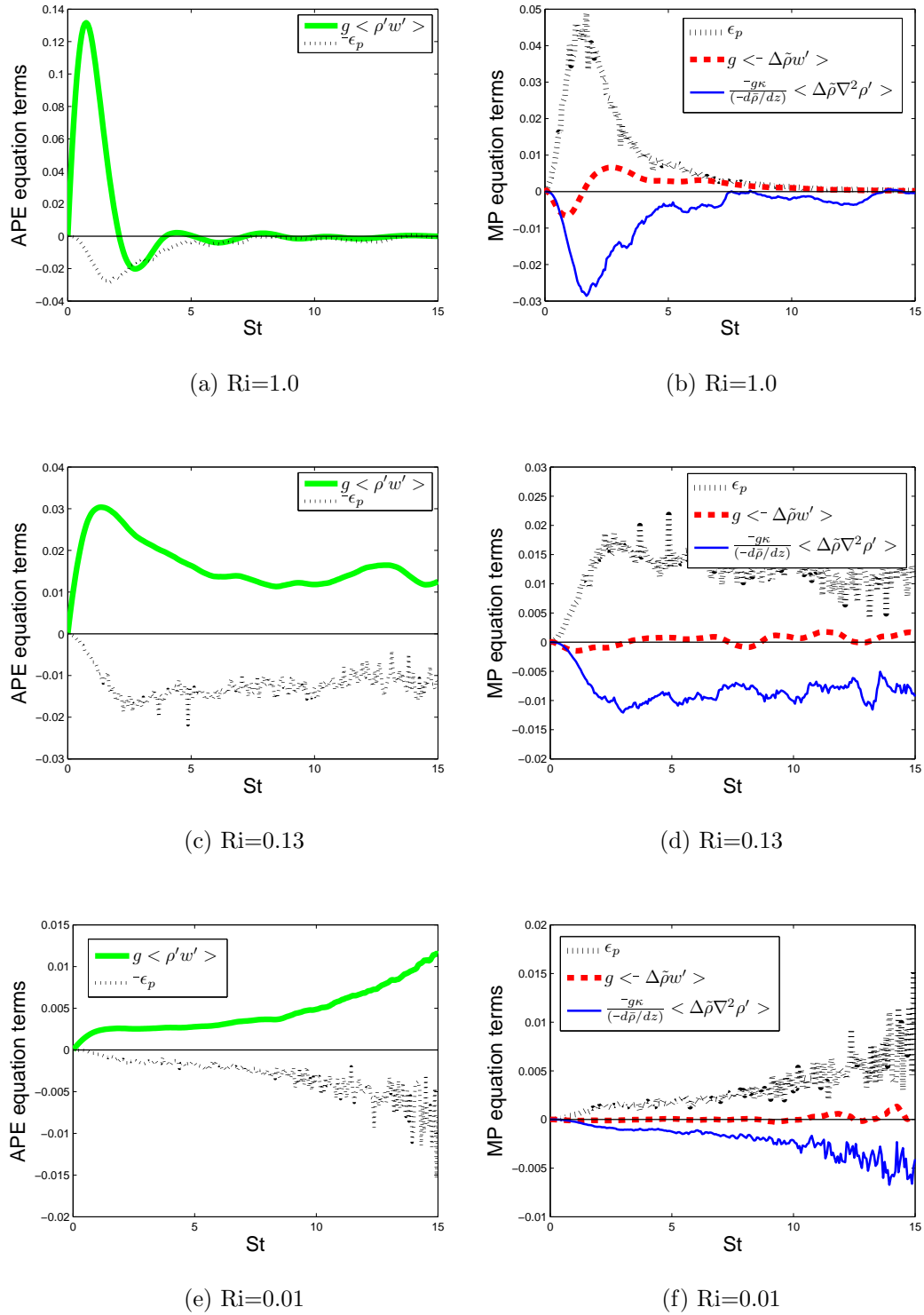
Figure 5.4: Time development of APE and MP evolution equation terms for (a), (b) Ri=1.0, (c), (d) Ri=0.13, (e), (f) Ri=0.01.
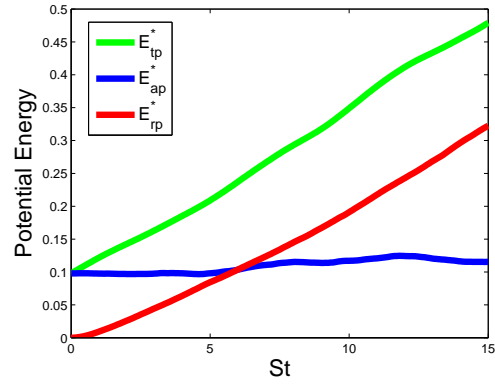
(a) TPE components
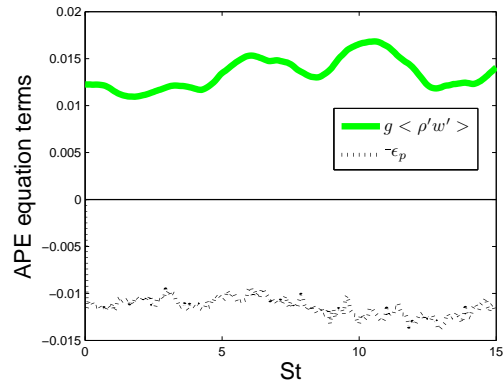
(b) APE equation terms
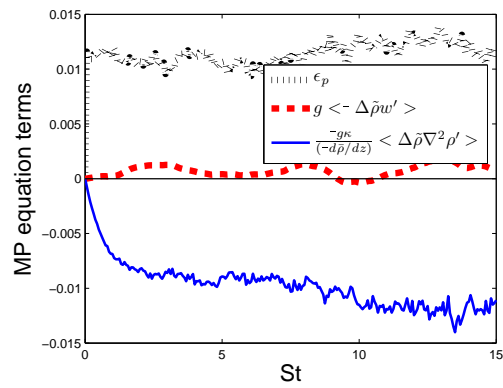
(c) MP equation terms

Figure 5.5: Time development of mean square vertical displacement and components for (a) TPE components, (b) APE equation terms, (c) MP equation terms.
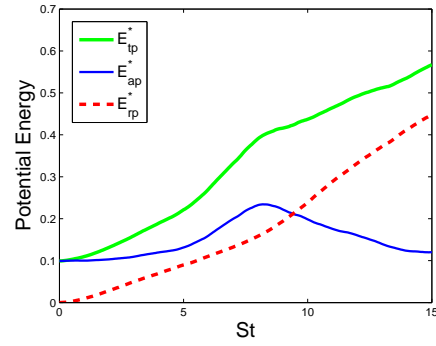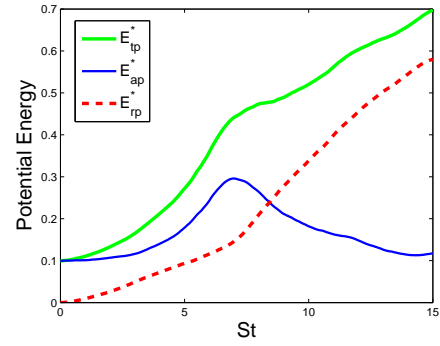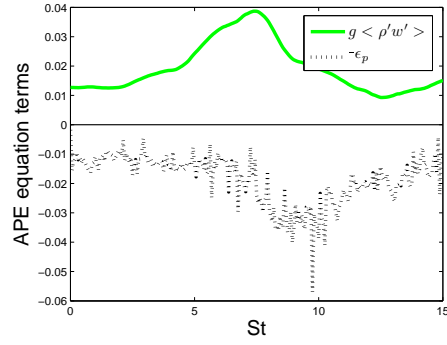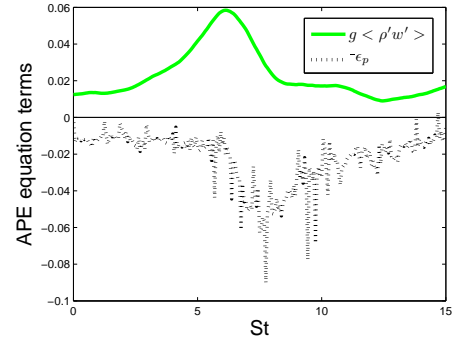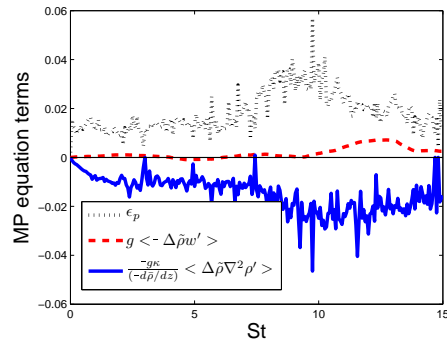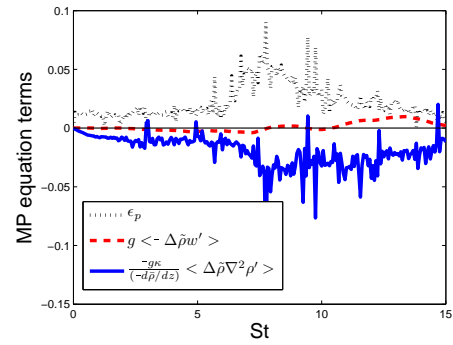
(a) high $\rho'w'$, TPE components

(b) high $\rho'\kappa\nabla^2\rho'$, TPE components

(c) high $\rho'w'$, APE equation

(d) high $\rho'\kappa\nabla^2\rho'$, APE equation

(e) high $\rho'w'$, DPE equation

(f) high $\rho'\kappa\nabla^2\rho'$, DPE equation

Figure 5.6: Time development of TPE components and evolution equation terms with conditional sampling ($St_c = 7.5$)
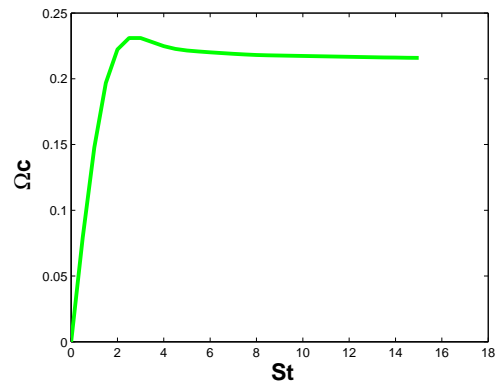
(a) Ri=1.0

(b) Ri=0.13
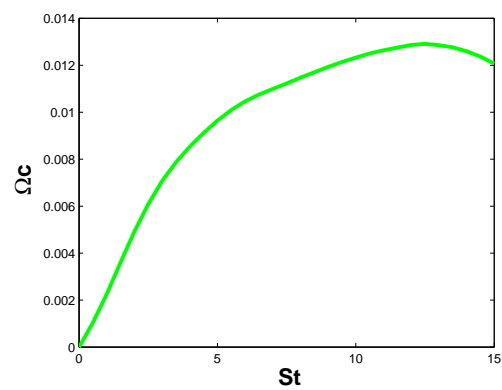
(c) Ri=0.01

Figure 5.7: Cumulative mixing efficiency, $\Omega_c(t)$, for (a) Ri=1.0, (b) Ri=0.13, (c) Ri=0.01
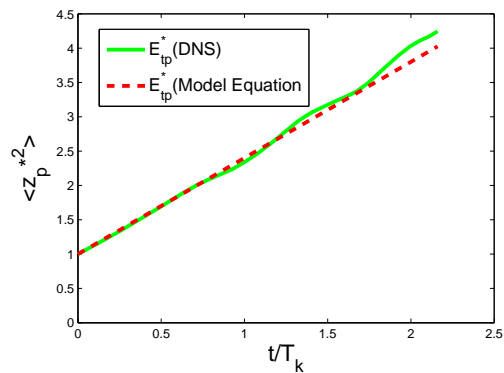
(a) Linear plot
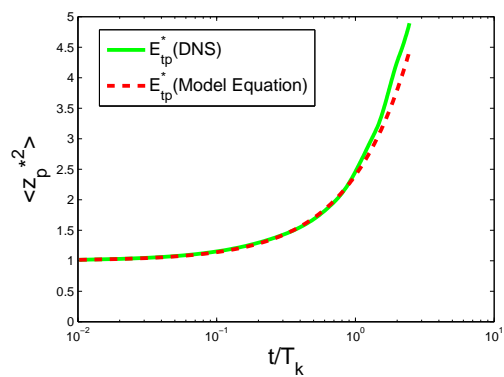
(b) Log-linear plot
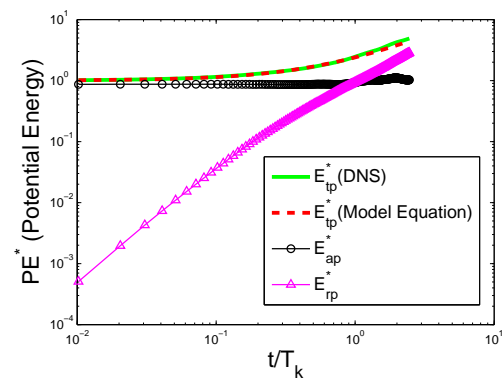
(c) Log-log plot

Figure 5.8: Vertical dispersion results and comparison with developed model for stationary shear flow(a) Linear plot, (b),(c) Log scale plots
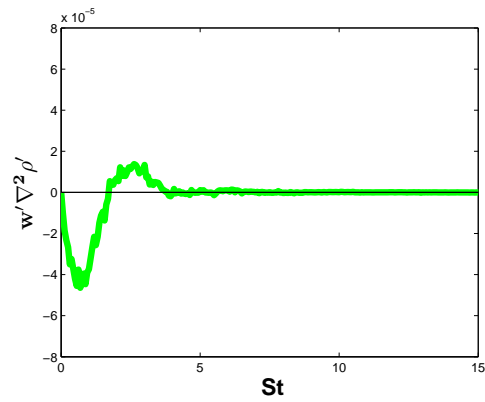
(a) Ri=1.0
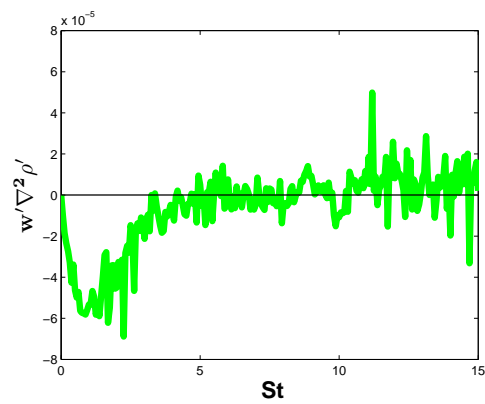
(b) Ri=0.13
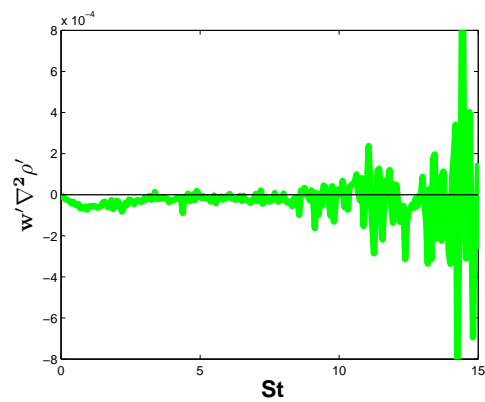
(c) Ri=0.01

Figure 5.9: Correlation between vertical velocity and mixing ($< w'\nabla^2\rho' >$) for (a) Ri=1.0, (b) Ri=0.13, (c) Ri=0.01.

Chapter 6

Conclusions

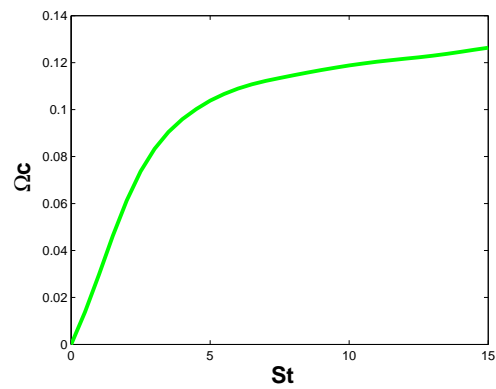This chapter presents a brief summary and discussion of the results and a brief suggestion for future work.

6.1   Summary of Research Study

The overall objective of this research is to study the fundamental physics of turbulent dispersion in stably stratified flows. We have developed an analysis framework which describes vertical dispersion in stably stratified homogeneous turbulence in terms of energetics in the Lagrangian frame. This allows us to clarify the ideas proposed by PPH and in particular, the transport mechanisms and the role and significance of molecular diffusion. Our analysis considers the total potential energy of a fluid particle TPE associated with the mean square vertical displacement, σ_{zp}^2, in terms of the available potential energy APE, associated with

non-equilibrium displacement, and the reference potential energy RPE, associated with changes in particle equilibrium height, i.e., equilibrium displacement. These energy quantities and their corresponding evolution equations describe the behavior of $\sigma_{zp}^2(t)$. As fluid particles move away from their equilibrium height, vertical kinetic energy is converted (reversibly) to APE. This establishes nonequilibrium displacement, z' and increases TPE. Without molecular diffusion, gravity will reduce the vertical velocity and the particles will tend to return to their original equilibrium height; APE is converted back to KE in this reversible process. With molecular diffusion, fluid particles will change their density, such to reduce ρ', and therefore, change their equilibrium height, i.e., some of the APE is dissipated and converted to RPE where it accumulates. Molecular diffusion thereby acts to *preserve displacements* and reduce the reconversion of PE to KE. In this manner, fluid particles can move further away from their original equilibrium level and $\sigma_{zp}^2(t)$ can grow without limit.

As discussed, the decomposition of the TPE (4.5) is essentially equivalent to that used by PPH and VS for total particle displacement. VS consider the relative significance of molecular mixing on dispersion by comparing the relative magnitudes of the *isopycnal displacment* (z'^2) and the *diapycnal displacement* (Δz_{eq}^2) with respect to z_p^2. They note that beyond the initial transient, Δz_{eq}^2 dominates in their decaying flows, even in weak stratification. Our analysis provides a clearer interpretation of these results by considering the associated energy quantities and corresponding evolution equations. The analysis shows that the molecular mixing

essentially redistributes energy between APE and RPE; TPE does not increase and the energy through transitory APE (z'^2) is stored as RPE (Δz_{eq}^2). We observe TPE (z_p^2) is dominated by RPE (Δz_{eq}^2) at long time for all cases, decaying, stationary and growing turbulence, from both of analytical results and DNS simulation results. However, since the increase in RPE is a direct result of energy conversion through APE, it does not dominate in the dynamical sense. In decaying turbulence, APE will eventually decay and what remains is the RPE accumulated during the transient event. The mean square vertical displacement σ_{zp}^2 equals the mean square equilibrium displacement $\langle \Delta z_{eq}^2 \rangle$ and approaches to a constant value given by the cumulative mixing efficiency $\Omega_c(\infty)$. In stationary turbulence, APE is maintained constant while RPE continually accumulates and grows. The mean square vertical displacement grows linearly in time at a rate given by the (constant) instantaneous mixing efficiency.

In general, the importance of these fully coupled effects between the velocity and scalar (density) fields depends on the strength of stratification. As stratification increases, buoyancy limits fluid particle advection thereby limiting TKE conversion to APE, and consequently to RPE. Vertical displacements are reduced, however, the relative significance of small-scale mixing with respect to the overall energetics becomes greater as indicated by the higher mixing efficiency, Ω_c.

The energetic analysis provides proper timescales associated with turbulent dispersion whereas one key assumption in PPH model is that small scale mixing is controlled by buoyancy time scale. The timescale for density changes due to

small scale mixing is found to be approximately insensitive to buoyancy and is determined by the turbulent decay time scale at large time. Hence the time scale for density changes is independent of stratification (N) and related to decay time scale, $\gamma' = \frac{1}{2}\frac{T_k}{T_\rho}$, where T_k is the decay time scale for TKE and T_ρ is the decay timescale for density fluctuations. Our proposed dispersion model based on this timescale agrees well with DNS results and provide substantial improvements over previous models.

6.2   Suggestions for Future Work

During our study, several interesting issues have been suggested from other researchers. In this study, we developed the general equations of Lagrangian energetics and then applied to an uniform stratified flow. However, the effect of non-uniform stratification ($\frac{d\rho_r}{dz} \neq$ constant) is important in the lower atmosphere where temperature inversions develop near the ground and on the top boundary layer of the ocean [13]. Roullet and Klein [44] investigated the anharmonic effect defined as $E_{anh} = E_a - E_{QG}$ where E_{QG} is a quadratic form of APE due to an uniform density profile. Moreover, the reference density in the atmospheric boundary layer changes in time and the reference density in the ocean continuously changes everyday. Therefore, the effect of non-uniform stratification ($\frac{d\rho_r}{dz} \neq$ constant) and unsteady stratification ($\frac{d\rho_r}{dt} \neq 0$) on the vertical dispersion should be further investigated.

In this study, we considered the linear Boussinesq flow which volumetric expansion coefficient (α) is constant. According to Tailleux [50], if the volumetric expansion coefficient is not constant and function of the temperature, the expansion/compression pressure work term in internal energy equation will be also function of the correlation between $|\nabla T|^2$ and $\frac{d\alpha}{dT}$ and this term can be significantly larger in a strongly turbulent fluids which leads the change in internal energy will be significantly increased. For the investigation of the effect of these nonlinear terms on energy transfer, the Lagrangian energetics with nonlinear equation of state should be developed further.

Our study is based on a strong fundamental physics and theory and they are confirmed by DNS. However, DNS results alone may not be sufficient in understanding of energetics and turbulent dispersion. Experiments and field studies should be further compared with DNS results and theories.

Appendix A

Direct Numerical Simulation

The problem to be investigated is a turbulent flow field with uniform shear and uniform density stratification. This simplest form of the flow contains all basic physical mechanisms but is more accessible to numerical simulations. A summary of the numerical methods will be presented in this chapter.

A.1   Numerical Formulation

The Direct Numerical Simulations code DISTUF (Direct Simulations of Turbulent Flows) is used to solve the exact time-dependent three-dimensional governing equations. The simulations performed follow those of Gerz, Schumann and Elghobashi [12], which uses a combination of second-order finite difference and pseudo-spectral to model homogeneous, isotropic incompressible turbulence with stratification and shear.

A.1.1 Dimensionless Scalings

The non-dimensional fluctuating velocities, time, length, pressure and fluctuating temperature are defined following:

$$u_i^* \quad = \quad \frac{u_i^{'}}{U_{ref}} \tag{A.1}$$

$$t^* \quad = \quad \frac{t}{L/U_{ref}} \tag{A.2}$$

$$x_i^* \quad = \quad \frac{x_i}{L} \tag{A.3}$$

$$p^* \quad = \quad \frac{p'}{\rho_o U_{ref}^2} \tag{A.4}$$

$$T^* \quad = \quad \frac{T'}{T_{ref}} \tag{A.5}$$

where $U_{ref} = \Delta U$ for shear flow, L is the length of the computational domain and $T_{ref} = \Delta T$ for stratified flow

For computing purposes, the non-dimensional density gradient and non-dimensional shear rate are defined as:

$$S_\rho^* \quad = \quad \frac{L}{\Delta \rho}\frac{\overline{\rho}}{dz} = \frac{L}{\Delta T}\frac{\overline{T}}{dz} \tag{A.6}$$

$$S^* \quad = \quad \frac{L}{\Delta U}\frac{dU}{dz} = S\frac{L}{\Delta U} \tag{A.7}$$

where $\frac{d\overline{\rho}}{dz}$ is the mean vertical density gradient and $S = \frac{dU}{dz}$ is the mean vertical velocity gradient. In the simulation, $S_\rho^* = 0$ for unstratified flow , $S_\rho^* = 1$ for stratified flow, $S^* = 0$ for unshear flow and $S^* = 1$ for shear flow.

A.1.2 Nondimensional Parameters

Relevant nondimensional parameters in this study are investigated.

The Reynolds number

The turbulent Reynolds number based on the Taylor microscale is defined as :

$$Re_\lambda \;=\; \frac{v\lambda}{\nu} \tag{A.8}$$

where ν is the kinematic viscosity, v is the root-mean-square of turbulent fluctuation velocity $(v = \sqrt{\frac{1}{3}(u_1^2 + u_2^2 + u_3^2)})$ and λ is the turbulent Taylor microscale.

The Shear number

The strength of the shear rate is characterized by the shear number and defined as :

$$Sh \;=\; S\frac{E_k}{\varepsilon_k} \tag{A.9}$$

where E_k is the turbulent kinetic energy (TKE) and ε_k is the dissipation of TKE

The Prandtl number

The Prandtl number is defined as the ratio of momentum diffusivity to thermal diffusivity.

$$Pr \;=\; \frac{\nu}{\kappa} \tag{A.10}$$

where κ is the thermal diffusive coefficient

Buoyancy Frequency

The strength of stratification is characterized by the buoyancy frequency and defined as :

$$N^2 \;=\; -\frac{g}{\rho_o}\frac{d\rho}{dz} \;=\; \alpha g \frac{dT}{dz} \tag{A.11}$$

In the simulation of this study, the density gradient is linear and N has a constant value.

The Richardson number

The relative significance of stratification to mean shear effects is characterized by the gradient Richardson number and defined as :

$$Ri \;=\; \frac{N^2}{S^2} \tag{A.12}$$

The flow regime are divided into three flow conditions by using the critical $Ri \approx$ 0.13. $Ri < 0.13, Ri = 0.13, Ri > 0.13$ regimes are respectively subcritical, critical and supercritical and each flow conditions corresponds to growing, stationary and decaying turbulence.

Shear and Buoyancy Time Scale

The shear and buoyancy time scale is respectively defined as St and Nt.

$$St \;=\; \frac{dU}{dz}\frac{L}{U_{ref}}t^* \;=\; \frac{dU}{dz}\frac{L}{\Delta U} \;=\; t^* \tag{A.13}$$

$$Nt \;=\; \frac{N}{S}St \;=\; \sqrt{Ri}\,t^* \tag{A.14}$$

A.1.3   Dimensionless Form of Governing Equations

Continuity Equation

The non-dimensionalized continuity equation is derived by substituting (A.5) to (2.20).

$$\frac{\partial u_i^*}{\partial x_i^*} = 0 \tag{A.15}$$

Momentum Equation

The non-dimensionalized momentum equation is derived by substituting (A.5), (3.20), (2.3) and (A.15) to (2.21).

$$\frac{\partial u_i^*}{\partial t^*} + \frac{\partial(u_i^* u_j^*)}{\partial x_j^*} + S^* x_3^* \frac{\partial u_i^*}{\partial x_1^*} + S^* u_3^* \delta_{i1} = -\frac{\partial p^*}{\partial x_i^*} + \frac{1}{Re}\frac{\partial^2 u_i^*}{\partial x_j^{*2}} + Ri T^* \delta_{i3} \tag{A.16}$$

Energy Equation

The non-dimensionalized energy equation is derived by substituting (A.5), (3.20) and (2.3) to (2.16).

$$\frac{\partial T^*}{\partial t^*} + \frac{\partial(u_j^* T^*)}{\partial x_j^*} + S_\rho^* x_3^* \frac{\partial T^*}{\partial x_1^*} = \frac{1}{RePr}\frac{\partial^2 T^*}{\partial x_j^{*2}} \tag{A.17}$$

A.1.4   Finite Difference Formulation

The computational domain considered in this study is a finite parallelepiped domain with streamwise, spanwise and vertical dimensions of length L. Each length section L has N grids of equal spacing Δx in all directions.

The governing equations are discretized by using a second-order accurate finite difference scheme except for the mean advection term where Fourier approximation is used. A second order accurate explicit Adams-Bashforth scheme is used to advance the discretized equations in time. The numerical scheme for integrating the velocity from time t^n to t^{n+1} proceeds in the following steps [12]:

1. The momentum equation is written in semi-discretized form as

$$\frac{u_i^{n+1} - u_i^n}{\Delta t} = r_i - \delta_i p \qquad (A.18)$$

   where r_i represents the convective and diffusive terms of the i-th velocity equation :

$$r_i = -\delta_j(\overline{u_i^j}\overline{u_j^i}) + \frac{1}{Re}\delta_j\delta_j u_i + Ri\overline{T}^3\delta_{i3} - S^*\overline{u_3}^3\delta_{i1} \qquad (A.19)$$

2. The value u_i^{n+1} at the next time stop is evaluated from :

$$u_i^{n+1} = u_i^n + \Delta t(r_i - \delta_i p) \qquad (A.20)$$

3. Applying the Adams-Bashforth time differencing scheme provides an intermediate value:

$$u_i^* = u_i^n + \Delta t(\phi_1 r_i^n - \phi_2 r_i^{n-1}) \qquad (A.21)$$

   The calculation is initiated at $n = 0$ with $\phi_1 = 1$, $\phi_2 = 0$. Then for $n > 0$, $\phi_1 = 3/2$, $\phi_2 = 1/2$

4. In the presence of shear, the next refinement of the velocity is obtained by evaluating u_i^*, initially obtained at position x, from where it is advected by the mean velocity Sx_3 during the timestep Δt. Fourier interpolation must be used to accurately obtain the refined estimation as the location x_1 does not necessary coincide with a grid point.

$$\widetilde{u}_i \;=\; u_i^*(x_1 - \Delta t S x_3) \tag{A.22}$$

5. The final step updates the intermediate value by :

$$u_i^{n+1} \;=\; \widetilde{u}_i - \Delta t \delta_i p^{n+1} \tag{A.23}$$

6. An implicit Poisson equation is obtained from (A.23) and (A.15)

$$\delta_i \delta_i p^{n+1} \;=\; \frac{\delta_i \widetilde{u}_i}{\Delta t} \tag{A.24}$$

p^{n+1} is obtained by Fast Fourier Transforms (FFT) algorithm and a Gaussian elimination.

A.1.5 Boundary Conditions

The periodic boundary conditions are implemented in the x_1 (streamwise) and x_2 (spanwise) directions and the shear periodic boundary condition is used in x_3 (vertical) direction [12]. The boundary conditions for any fluctuation f

$$f(x_1 + m_1 l_1, x_2 + m_2 l_2, x_3 + m_3 l_3) \;=\; f(x_1 - S m_3 l_3 t, x_2, x_3) \tag{A.25}$$

where m_i are arbitrary integers and l_i are nondimensional domain lengths

A.1.6   Initial Conditions

The velocity $u_i(x_i, t)$ has a finite Fourier transform representation, with N^3 corresponding discrete nodes in the wavenumber space. The lowest nonzero wavenumber is $k_0 = \frac{2\pi}{L}$. The components of the wavenumber vector k_i at a given node are integer multiples of k_0 ranging from $k_{min} = (1 - \frac{1}{2}N)k_0$ to $k_{max} = \frac{1}{2}Nk_0$ [72]. Simulations are initialized with fully developed isotropic turbulent velocity field. A random number generator is used to produce the initial fluctuating fields that contain no phase information and no initial spectral transfer [21]. This initial velocity field satisfies the equation of continuity and governed by a prescribed three-dimensional energy spectrum $E(k, 0)$ of random and uncorrelated phase:

$$E(k, 0) \quad = \quad \left(\frac{3v_0^2}{2}\right)\left(\frac{k}{k_p^2}\right)e^{\left(-\frac{k}{k_p}\right)} \tag{A.26}$$

where k_p is the wavenumber of the spectrum peak and v_0 is the initial rms velocity. This spectrum function is associated with the initial period of decay for isotropic turbulence, which is characterized by a relatively higher energy content at the lower wavenumbers. In this study, $k_p = 6(2\pi)$ is chosen which is large enough for the integral lengthscale to grow during the simulation period and small enough for the energy and dissipation rates to be sufficiently small at the largest resolved wavenumber k_{max} [12]. The initial total energy is exclusively kinetic in form, as the initial temperature fluctuations are set to zero.

The initial spectra are chosen to allow a parameterization of the flow evolution based on the specific set of initial conditions but this initial state is not

sufficient to contain the energy in the lowest and highest wavenumber portions of spectrum due to a strong increase in the viscous dissipation, hence, a large drop of turbulent kinetic energy, turbulent Reynolds number and shear number. An alternative initialization method is introduced by Jacobitz *et al.*[21] to reduce the initial drop of these values. A preliminary simulation is performed in advance for about one eddy-turnover time ($St = 2$) for the initially random, unstratified, un-sheard isotropic turbulent velocity fields to become fully developed with necessary phase correlation as dictated by the Navier-Stokes equations. The initial energy spectrum evolves into a spectrum characteristics for fully developed turbulent flow : the low wavenumber portion gains energy and the high wavenumber portion loses energy, but the general shape of the spectrum changes slightly. The skewness of the velocity derivative is a measure of the nonlinear energy transfer from low to high wavenumbers:

$$
S_u \quad = \quad \sum_{i=1}^{3} \frac{\frac{1}{3}\langle\left(\frac{\partial u_i}{\partial x_i}\right)^3\rangle}{(\frac{1}{3}\langle\left(\frac{\partial u_i}{\partial x_i}\right)^3\rangle)^{\frac{3}{2}}} \tag{A.27}
$$

The initial skewness is zero, which corresponds to the initial random isotropic velocity field with no energy transfer. After a short initial period, it increases to an asymptotic value and the preliminary simulation is ended as turbulence can be regarded as fully developed. The initial values of the Reynolds number and shear number of this first preliminary simulation are chosen so that the values at the end of this simulation match the target initial set of parameters of the actual simulation [21]. Buoyancy and shear are introduced to flow after the preliminary

simulation has done at $St = 2$. The fluid particles are also released into the flow at the end of the preliminary simulation as turbulence evolves to the beginning of the asymptotic region.

A.2   Particle Tracking Algorithm

In the Lagrangian frame, a large number of tagged fluid particles are tracked as the Eulerian flow field evolves. In order to gain Lagrangian statistics, a particle tracking algorithm is used [61]. Denoting $x_i(x_{0i}, t)$ and $u_i(x_{0j}, t)$ as the position and velocity at time t of a fluid particle in the Lagrangian viewpoint with initial position x_0 at time t=0, the equations of motion of the fluid particle is given by:

$$\frac{\partial x_i(x_{0i}, t)}{\partial t} = u_i(x_{0j}, t) \tag{A.28}$$

The Lagrangian velocity $u_i(x_{0j}, t)$ is determined from the spatial Eulerian velocity field by

$$u_i(x_{0j}, t) = u_i(x_k(x_{0j}, t), t) = U_1(x_3) + u'_i(x_j, t) \tag{A.29}$$

A.2.1   Time Integration of Particle Motion

From DNS, the Eulerian velocity u_i is available at every grid point in 3-D computational domain at each time step. Interpolation scheme is required to determine the velocity at any arbitrary position within the field. After the release of fluid particles, (A.28) is integrated for the first time advancement using the

Euler scheme:

$$x_i(t^1) \quad = \quad x_i(t^0) + \Delta t u_i'(t^0) + \Delta U_1(x_3(t^0))\delta_{i1} \qquad (A.30)$$

and thereafter by a second-order accurate Adams-Bashforth scheme in each coordinate direction [61]:

$$x_i(t^{n+1}) \quad = \quad x_i(t^n) + \frac{\Delta t}{2}\left[3u_i'(t^n) - u_i'(t^{n-1})\right] + \Delta t U_1(x_3(t^n))\delta_{i1} \quad (A.31)$$

where $U_1(x_3)\delta_{i1}$ is the local mean velocity of the particle and Δt is the constant timestep chosen in accordance with that used in the integration of Navier Stokes equations. The particle trajectory does not coincide with the grid points where the fluid velocity is known, hence u_i has to be interpolated to the particle's position so that it can be advanced to its next new position [58].

A.2.2 Velocity Interpolation

The fluid particle velocity is an essential parameter to determine Lagrangian statistics. Different interpolation schemes can be used to obtain the particle velocities. For a numerical accuracy and computational efficiency, two interpolation schemes, ordinary linear interpolation scheme and cubic spline interpolation scheme, are used. The linear interpolation scheme is considered initially because of its simplicity.

The cubic spline interpolation scheme follows the formulation given by Yeung and Pope [71]. It has the distinct advantages of fourth-order accuracy and

twice-continuously differentiable approximations. There are essentially two main steps in cubic spline interpolation schemes :

The first step is to evaluate the cubic spline coefficients, e_i. The basis functions and their coefficients are also considered to be continued periodically outside the interval because the velocity fields from the Eulerian DNS are periodic [61]. For DNS calculations of N equispaced nodes in each direction, $N_b = N + 3$ basis functions are required to locate at the nodes and their periodic extensions, one extended basis function to the left of the first node and two basis functions to the right of the Nth node. The periodic velocity function can be extended to have $N + 3$ collocation points, hence the cubic spline coefficients can be determined from the N_b collocation conditions.

$$\sum_{j=1}^{N} T_{ij} e_j \quad = \quad u_i \ \text{ for } \ i = 0, ..., N_b \qquad (A.32)$$

where

$$T_{ij} = \begin{cases} \frac{2}{3} & \text{for } \ i = j \\ \frac{1}{6} & \text{for } \ |i - j| = 1 \\ \frac{1}{6} & \text{for } \ (i, j) = (1, N) \ \text{ or } \ (N, 1) \\ 0 & \text{otherwise} \end{cases} \qquad (A.33)$$

The second step is to perform the interpolation.

$$g(x) \quad = \quad \sum_{i=0}^{N_b - 1} b_i(x) e_i \qquad (A.34)$$

where $b_i(x)$ is the ith basis function. At any given location, only four basis functions are nonzero. Numbering the nodal points from x_1 to x_N and defining $\Delta x =$

$x_1 - x_0 = x_{N+1} - x_N$ and $\xi = \frac{x - x_i}{\Delta x}$ for $i = 0, 1, ...N + 1, N + 2$, the ith basis function at any given position x is given by :

$$b_i(x) = \begin{cases} \frac{1}{6}(2 + \xi)^3 & \text{for } -2 \le \xi \le -1 \\ \frac{1}{6}(-3\xi^3 - 6\xi^2 + 4) & \text{for } -1 \le \xi \le 0 \\ \frac{1}{6}(3\xi^3 - 6\xi^2 + 4) & \text{for } 0 \le \xi \le 1 \\ \frac{1}{6}(2 - \xi)^3 & \text{for } 1 \le \xi \le 2 \\ 0 & \text{otherwise} \end{cases} \quad (A.35)$$

The three-dimensional spline can be represented as the tensor product of three one-dimensional splines as follow:

$$u(x_1, x_2, x_3) = \sum_{k=0}^{N_b-1} \sum_{j=0}^{N_b-1} \sum_{i=0}^{N_b-1} b_i(x_1)c_j(x_2)d_k(x_3)e_{ijk} \quad (A.36)$$

where b_i, c_j and d_k are the one-dimensional basis functions in the x_1, x_2 and x_3 coordinate directions respectively. (A.36) can be decomposed as:

$$u(x_{1I}, x_{2J}, x_{3K}) = \sum_{i=0}^{N_b-1} b_i(x_{iI})E_{iJK} \quad (A.37)$$

where

$$E_{iJK} = \sum_{j=0}^{N_b-1} c_j(x_{2J})F_{IjK} \quad (A.38)$$

$$F_{IjK} = \sum_{k=0}^{N_b-1} d_k(x_{3K})e_{ijk} \quad (A.39)$$

From (A.37), (A.38) and (A.39), N_b^3 cubic spline coefficients can be obtained.

A.2.3 Particle Sampling Size

From the central limit theorem, the relative error of an ensemble average varies as $N_{PART}^{-\frac{1}{2}}$ where N_{PART} is the number of particles used in the simulation. For a statistically homogeneous flow filed, Eulerian statistics obtained from volume averaging over all grid points are equivalent to Lagrangian statistics obtained from ensemble averaging over all fluid particles. VS [62] show that the sample size of 8^3 particles is sufficient to obtain the accurate Lagrangian statistics. For this study, Lagrangian statistics is obtained from a set of 16^3 number of particles.

A.2.4 Resolution Requirement

DNS of turbulent flows is the numerical solution of the exact, three-dimensional, time-dependent Navier-Stokes equations in the absence of turbulence closure model or inevitable empiricism. Since no modeling assumptions are made, basic physics must be recovered directly from simulation results. Therefore, the size of the computational domain must be large enough to capture the largest turbulence scales, usually characterized by the integral length scale l. These requirements determine the number of necessary grid points N where N is the number of grid points. VS [62] show that the 64^3 grid resolution is sufficient to meet these requirements. In this study, based on current computer resources, resolution is limited to $N = 128$ and the total size of the computational domain is $N_{total} = N^3 = 128^3$.

Bibliography

[1] D. G. Andrews. A note on potential energy density in a stratified compressible fluid. *J. Fluid Mech.*, 107:227–236, 1981.

[2] P. R. Bannon. On the anelastic approximation for a compressible atmosphere. *J. Atmos. Sciences.*, 53:3618–3628, 1996.

[3] G. K. Batchelor. *An Introduction to Fluid Dynamics*. Cambridge University Press, New York, 1967.

[4] J. Boussinesq. Théorie analytique de la chaleur. *Gauthier-Villars.*, 2, 1903.

[5] G. Brethouwer and E. Lindborg. Numerical study of vertical dispersion by stratified turbulence. *J. Fluid Mech.*, 631:149–163, 2009.

[6] A. W. Cook and J. J. Riley. Direct numerical simulation of a turbulent reactive plume on a parallel computer. *J. Comput. Phys.*, 129:263–283, 1996.

[7] G.T. Csanady. Turbulent diffusion in a stratified fluid. *J. Atmos. Sci.*, 21:439–447, 1964.

[8] B. Cushman-Roisin. *Introduction to Geophysical Fluid Dynamics*. Prentice-Hall, Inc., New Jersey, 1994.

[9] S. K. Das and P. A. Durbin. A lagrangian stochastic model for dispersion in stratified turbulence. *Phys. Fluids*, 17:1–10, 2005.

[10] P. J. Diamessis and K. K. Nomura. The structure and dynamics of overturns in stably stratified homogeneous turbulence. *J. Fluid Mech.*, 499:197–229, 2004.

[11] D. R. Durran and A. Arakawa. Generalizing the boussinesq approximation to stratified compressible flow. *C. R. Mec.*, 335:655–664, 2007.

[12] T. Gerz, U. Schumann, and S. Elghobashi. Direct simulation of stably stratified homogeneous turbulent shear flows. *J. Fluid Mech.*, 200:563–594, 1989.

[13] A. E. Gill. *Atmosphere-Ocean Dynamics.* Academic Press, London, 1982.

[14] D. Holliday and M. E. McIntyre. On potential energy density in an incompressible, stratified fluid. *J. Fluid Mech.*, 107:221–225, 1981.

[15] S. E. Holt, J. R. Koseff, and J. H. Ferziger. A numerical study of the evolution and structure of homogeneous stably stratified sheared turbulence. *J. Fluid Mech.*, 237:499–539, 1992.

[16] G. O. Hughes and R. W. Griffiths. Horizontal convection. *Annu. Rev. Fluid Mech.*, 40:185–208, 2008.

[17] G. O. Hughes, A. M. Hogg, and R. W. Griffiths. Available potential energy and irrevisible mixing in the meridional overturning circulation. *J. Phys. Oceanogr.*, 39:3130–3146, 2009.

[18] J.C.R. Hunt. Diffusion in the stably stratified atmospheric boundary layer. *J. Clim. Appl. Met.*, 24:1187–1195, 1985.

[19] J.C.R. Hunt. Turbulent diffusion from complex flows. *Ann. Rev. Fluid. Mech.*, 17:447–485, 1985.

[20] F.G. Jacobitz and S. Sarkar. On the shear number effect in stratified shear flow. *Theor. Comput. Fluid Dyn.*, 13:171–188, 1999.

[21] F.G. Jacobitz, S. Sarkar, and C.W. Van Atta. Direct numerical simulations of the turbulence evolution in a uniformly sheared and stably stratified flow. *J. Fluid Mech.*, 342:231–261, 1997.

[22] Y. Kaneda and T. Ishida. Suppression of vertical diffusion in strongly stratified turbulence. *J. Fluid Mech.*, 402:311–327, 2000.

[23] D. Kang and O. Fringer. On the circulation of available potential energy in internal wave fields. *J. Phys. Oceanogr.*, 40:2539–2545, 2010.

[24] Y. Kimura and J.R. Herring. Diffusion in stably stratified turbulence. *J. Fluid Mech.*, 328:253–269, 1996.

[25] S. Klainerman and A. Majda. Compressible and incompressible fuids. *Commun. Pur. Appl. Math.*, 35:629–651, 1982.

[26] R. Klein. Semi-implicit extension of a godunov-type scheme based on low mach number asymptotics i: One-dimensional flow. *J. Comput. Phys.*, 121:213–237, 1995.

[27] K. P. Kundu and M. I. Cohen. *Fluid Mechanics.* Academic Press, London, 2008.

[28] K. G. Lamb. On the calculation of the available potential energy of an isolated perturbation in a density-stratified fluid. *J. Fluid Mech.*, 597:415–427, 2008.

[29] E. Lindborg and G. Brethouwer. Vertical dispersion by stratified turbulence. *J. Fluid Mech.*, 614:303–314, 2008.

[30] E. N. Lorenz. Available potential energy and the maintenance of the general circulation. *Tellus*, 7:157–167, 1955.

[31] E. N. Lorenz. *The Nature and Theory of the General Circulation of the Atmosphere.* World Meteorological Organization, Switzerland, 1967.

[32] M. Margules. *Über die energie der sturme (translation by c. abbe tyle, k. r. 1995. intense surface anticyclogenesis: clima- (1910) in smithsonian institute miscellaneous collec- tology and composite/individual case studies. m.sc. tion 51, 553.595). Jahrb. Zentralanst. Meteor.*, pages 1–26, 1903.

[33] M. J. Molemaker and J. C. McWilliams. Local balance and cross-scale flux of available potential energy. *J. Fluid Mech.*, 645:295–314, 2010.

[34] M. J. Moran, H. N. Shapiro, D. D. Boettner, and M. B. Bailey. *Fundamentals of Engineering Thermodynamics.* Wiley, New York, 2011.

[35] W. H. Munk and C. Wunsch. Abyssal recipes ii: energetics of tidal and wind mixing. *Deep Sea Res.*, 45:1997–2010, 1998.

[36] C. Nappo and P. Johanson. Turbulence and diffusion in the stable planetary boundary layer. Summary of Lovangan International Workshop, 1999.

[37] T. R. Osborn and C. S. Cox. Oceanic fine structure. *Geophys. Fluid Dyn.*, 3:321–345, 1972.

[38] R. L. Panton. *Incompressible Flow.* Wiley, New York, 1996.

[39] F. Paparella and W. R. Young. Horizontal convection is non-turbulent. *J. Fluid Mech.*, 466:205–214, 2002.

[40] H.J. Pearson, J.S. Puttock, and J.C.R. Hunt. A statistical model of fluid element motions and vertical diffusion in a homogeneous stratified turbulent flow. *J. Fluid Mech.*, 129:219–249, 1983.

[41] W. R. Peltier and C. P. Caulfield. Mixing efficientcy in stratified shear flows. *Annu. Rev. Fluid Mech.*, 35:135–167, 2003.

[42] S. B. Pope. The vanishing effect of molecular diffusivity on turbulent dispersion: implications for turbulent mixing and the scalar flux. *J. Fluid Mech.*, 359:299–312, 1998.

[43] F. Roquet. Dynamical potential energy: A new approach to ocean energetics. *J. Phys. Oceanogr.*, 43:457–476, 2013.

[44] G. Roullet and P. Klein. Available potential energy diagnosis in a direct numerical simulation of rotating stratified turbulence. *J. Fluid Mech.*, 624:45–55, 2009.

[45] J. W. Sandstrom. Dynamischhe versuche mit meerwasser. *Ann. Hydrodynam. Marine Meteorol*, 36:6–23, 1908.

[46] A. Scotti, R. Beardsley, and B. Butman. On the interpretation of energy and energy fluxes of nonlinear internal waves: an example from massachusetts bay. *J. Fluid Mech.*, 561:103–112, 2006.

[47] P. Shen and P. K. Yeung. Fluid particle dispersion in homogeneous turbulent shear flow. *Phys. Fluids*, 9:3472–3484, 1997.

[48] E. A. Spiegel and G. Veronis. On the boussinesq approximation for a compressible fluid. *Astrophys. Journal*, 131:442–447, 1960.

[49] M. W. Sverdrup, H. U. Johnson and R. H. Fleming. The oceans their physics, chemistry, and general biology. *Ann. Hydrodynam. Marine Meteorol*, 36:6–23, 1942.

[50] R. Tailleux. On the energetics of stratified turbulent mixing, irreversible thermodynamics, boussinesq models, and the ocean heat engine controversy. *J. Fluid Mech.*, 638:339–382, 2009a.

[51] R. Tailleux. Understandinf mixing efficiency in the oceans: do the nonlinearities of the equation of state for seawater matter? *Ocean science*, 5:271–283, 2009b.

[52] R. Tailleux. Thermodynamics/dynamics coupling in weakly compressible turbulent stratified fluids. *ISRN Thermodynamics*, 2012, 2012.

[53] R. Tailleux. Available potential energy and exergy in stratified fluids. *arf*, 45:35–58, 2013.

[54] R. Tailleux. Available potential energy density for a multicomponent boussinesq fluid with arbitrary nonlinear equation of state. *jfm*, 705:499–518, 2013.

[55] R. Tailleux. Irreversible compressible work and available potential energy dissipation in turbulent stratified fluids. *Phys. Scr.*, 2012, 2013.

[56] R. Tailleux and L. Rouleau. The effect of mechanical stirring on horizontal convection. *Dynamic Meteorology and Oceanography*, 62:138–152, 2010.

[57] G.I. Taylor. Diffusion by continuous movements. *Proc. R. Soc. London Ser.*, A 20:196–211, 1921.

[58] G. C. Truesdell. *The interaction between decaying isotropic turbulence and dispersed solid particles.* PhD thesis, University of California, Irvine, 1993.

[59] J. S. Turner. *Buoyancy effects in fluids.* Cambridge University Press, New York, 1973.

[60] M. van Aartrijk, H. J. H. Clercx, and K. B. Winters. Single-particle, particle-pair, and multiparticle dispersion of fluid particles in forced stably stratified turbulence. *Phys. Fluids*, 20(025104):1–16, 2008.

[61] S. K. Venayagamoorthy. Turbulent mixing and dispersion in environmental flows. Master's thesis, University of Natal, 2002.

[62] S. K. Venayagamoorthy and D. D. Stretch. Lagrangian mixing in decaying stably stratified turbulence. *J. Fluid Mech.*, 564:197–226, 2006.

[63] A. Venkatram, D. Strimaitis, and D. Dicristofaro. A semiempirical model to estimate vertical dispersion of elevated releases in the stable boundary layer. *Atmos. Environ.*, 18:923–928, 1984.

[64] W. Wang and R. X. Huang. An experimental study on thermal circulation driven by horizontal differenial heating. *J. Fluid Mech.*, 540:49–73, 2005.

[65] J. C. Weil. Updating applied diffusion models. *J. of Clim. and Appl. Met.*, 24(11):1111–1129, 1985.

[66] K. B. Winters and R. Barkan. Available potential energy density for boussinesq flow. *J. Fluid Mech.*, 714:476–488, 2013.

[67] K. B. Winters and E. A. D' Asaro. Diascalar flux and the rate of fluid mixing. *J. Fluid Mech.*, 317:179–193, 1996.

[68] K. B. Winters, P. N. Lombard, J. J. Riley, and E. A. D' Asaro. Available potential energy and mixing in density stratified fluids. *J. Fluid Mech.*, 289:115–128, 1995.

[69] K. B. Winters and W. R. Young. Available potential energy and buoyancy variance in horizontal covection. *J. Fluid Mech.*, 629:221–230, 2009.

[70] C. Wunsch and R. Ferrari. Vertical mixing, energy, and the general circulation of the oceans. *Annu. Rev. Fluid Mech.*, 36:281–314, 2004.

[71] P. K. Yeung and S. B. Pope. An algorithm for tracking fluid particles in numerical simulations of homogeneous turbulence. *Phys. Fluids*, 79:373–416, 1988.

[72] P. K. Yeung and S. B. Pope. Lagrangian statistics from direct numerical simulations. *J. Fluid Mech.*, 207:531–586, 1989.

[73] W. R. Young. Dynamic enthalpy, conservative temperature, and the seawater boussinesq approximation. *J. Phys. Oceanogr.*, 40:394–400, 2010.